

Evaluation of CORDEX ERA5-forced ‘NARClIM2.0’ regional climate models over Australia using the Weather Research and Forecasting (WRF) model version 4.1.2

Giovanni Di Virgilio^{1,2}, Fei Ji^{1,3}, Eugene Tam¹, Jason P. Evans^{2,3}, Jatin Kala⁴, Julia Andrys⁴, Christopher Thomas², Dipayan Choudhury¹, Carlos Rocha¹, Yue Li¹, and Matthew L. Riley¹

¹Climate & Atmospheric Science, NSW Department of Planning and Environment, Sydney, Australia

²Climate Change Research Centre, University of New South Wales, Sydney, Australia

³Australian Research Council Centre of Excellence for Climate Extremes, University of New South Wales, Sydney, Australia

⁴Environmental and Conservation Sciences, and Centre for Climate Impacted Terrestrial Ecosystems, Harry Butler Institute, Murdoch University, Murdoch, WA 6150, Australia

Correspondence to: Giovanni Di Virgilio (giovanni.divirgilio@environment.nsw.gov.au; giovanni@unsw.edu.au)

1 **Abstract.** Understanding regional climate model (RCM) capabilities to simulate current climate
2 informs model development and climate change assessments. This is the first evaluation of the
3 NARClIM2.0 ensemble of seven Weather Forecasting and Research RCMs driven by ECMWF
4 Reanalysis v5 (ERA5) over Australia at 20 km resolution contributing to CORDEX-CMIP6
5 Australasia, and south-eastern Australia at convection-permitting resolution (4 km). The performances
6 of these seven ERA5-RCMs (R1-R7) in simulating mean and extreme maximum, minimum
7 temperature and precipitation is evaluated against observations at annual, seasonal, and daily
8 timescales, and compared to corresponding performances of previous-generation CORDEX-CMIP5
9 Australasia ERA-Interim-driven RCMs. ERA5-RCMs substantially reduce cold biases for mean and
10 extreme maximum temperature versus ERA-Interim-RCMs, with the best-performing ERA5-RCMs
11 showing small mean absolute biases (ERA5-R5: 0.54K; ERA5-R1: 0.81K, respectively), but produce
12 no improvements for minimum temperature. At 20 km resolution, improvements in mean and extreme
13 precipitation for ERA5-RCMs versus ERA-Interim RCMs are principally evident over south-eastern
14 Australia, whereas strong biases remain over northern Australia. At convection-permitting scale over
15 south-eastern Australia, mean absolute biases for mean precipitation for the ERA5-RCM ensemble are
16 around 79% smaller versus the ERA-Interim RCMs that simulate for this region. Although ERA5
17 reanalysis data confer improvements over ERA-Interim, only improvements in precipitation

18 simulation by ERA5-RCMs are attributable to the ERA5 driving data, with RCM improvements for
19 maximum temperature more attributable to model design choices, suggesting improved driving data
20 do not guarantee all RCM performance improvements, with potential implications for CMIP6-forced
21 dynamical downscaling. This evaluation shows that NARClIM2.0 ERA5-RCMs provide valuable
22 reference simulations for upcoming CMIP6-forced downscaling over CORDEX-Australasia and are
23 informative datasets for climate impact studies. Using a subset of these RCMs for simulating CMIP6-
24 forced climate projections over CORDEX-Australasia and/or at convection-permitting scales could
25 yield tangible benefits in simulating regional climate.

Keywords:

26 Climate change; climate impact adaptation; CORDEX-CMIP6; dynamical downscaling; model
27 development; reanalysis

28 **1. Introduction**

29 Global climate models (GCMs) are optimum tools for simulating future climate at global and
30 continental scales, informing policy and planning at these scales on climate change under different
31 greenhouse gas concentration scenarios (IPCC, 2021). Successive generations of GCMs have seen
32 several improvements, including incremental increases in spatial resolution and some improvements
33 in the simulation of the current climate (Eyring et al., 2016; Stouffer et al., 2017; Grose et al., 2020).
34 However, the coarse spatial resolution of GCMs (100 to 250 km) limits their ability to resolve the
35 fine-scale drivers of regional climate, such as complex topography, land-use, and mesoscale
36 atmospheric processes like convection. This in turn limits their efficacy for climate mitigation and
37 adaptation planning at regional scales (Hsiang et al., 2017).

38 Dynamical downscaling of GCM outputs using regional climate models (RCMs) is one
39 approach for generating high-resolution climate projections at regional scales (Giorgi, 2006; Laprise,
40 2008). RCMs use GCM outputs as initial and lateral boundary conditions to generate fine-scale
41 climate simulations that better resolve the fine-scale drivers of regional climate (Giorgi and Bates,
42 1989; Torma et al., 2015; Di Luca et al., 2012). This can create fine-scale climate information that is
43 spatially and temporally more realistic than the driving GCM information, providing climate
44 simulations more suitable for regional climate impact studies (Giorgi, 2019). However, such
45 improvements are not guaranteed, and typically vary with time and location (Di Virgilio et al., 2019;
46 Di Virgilio et al., 2020b; Panitz et al., 2014; Bucchignani et al., 2016). There is also the potential that
47 RCMs simulate climate projections that are not more physically plausible than those of driving GCMs
48 (Ekström et al., 2015). Design considerations such as selection of driving models and RCM
49 parameterisation also underlie the nature of potential improvements in regional climate simulations.

50 The Coordinated Regional Climate Downscaling Experiment (CORDEX) is an initiative of the
51 World Climate Research Programme (WCRP) that provides experimental guidelines facilitating both
52 the production of regional climate projections, and inter-model comparisons across modelling groups
53 (Giorgi et al., 2009). Under CORDEX, regional climate projections based on CMIP5 (Coupled Model
54 Intercomparison Project Phase 5) GCM projections were produced for fourteen regions globally.
55 CORDEX is building on these previous downscaling intercomparison projects to provide a common
56 framework for downscaling activities based on CMIP6 GCMs (Gutowski et al., 2016).

57 A key component of CORDEX is using RCMs to dynamically downscale reanalyses such as
58 ERA-Interim (Dee et al., 2011) under CORDEX-CMIP5, and recently ERA5 (Hersbach et al., 2020)
59 under CORDEX-CMIP6, and evaluating the RCMs' capabilities to simulate present-day climate. If a
60 given RCM performs poorly in simulating the present-day climate, this lowers confidence in future
61 climate changes projected by this model. Assessing the relative strengths and weaknesses of ERA5-
62 forced RCMs can inform the decision to exclude poorer performing RCM configurations when selecting

63 a subset of RCMs for downscaling of CMIP6 GCMs. It also helps benchmark the subsequent
64 performance profiles of CMIP6-forced RCM projections and hindcasts.

65 Previous work to dynamically downscale ERA5 over CORDEX Australasia includes the
66 BARPA-R (Bureau of Meteorology Atmospheric Regional Projections for Australia) regional climate
67 model which simulates over CORDEX Australasia at ~17 km resolution (Howard et al., 2024).
68 Evaluation of BARPA-R's skill in simulating the Australian climate observed good performance
69 overall, including a 1°C cold bias in daily maximum temperatures and wet biases of up to 25 mm/month
70 over inland Australia. Other previous studies of dynamical downscaling of ERA5 by RCMs have
71 focused on short-term (e.g. ~one year) regional climate simulations (e.g. Varga and Breuer, 2020; Zhou
72 et al., 2021) rather than multidecadal simulations. Several have focused on specific regions that are not
73 CORDEX domains, some of which have a smaller spatial extent in comparison. For instance, Reder et
74 al. (2022) conducted dynamical downscaling of ERA5 using COSMO-CLM (CCLM; Rockel et al.
75 2008) on nine separate domains over twenty European cities at convection-permitting scale (~2.2 km).
76 They demonstrated an overall pattern of added value in the simulation of heavy precipitation at city
77 scale relative to the driving reanalysis. Focusing on precipitation simulation over the Lake Victoria
78 Basin in Africa, Van De Walle et al. (2020) conducted ERA5-forced CCLM simulations at convection-
79 permitting scale. They found that CCLM outperformed the ERA5 data set, as well as RCM simulations
80 using parametrised convection, though a domain-averaged wet bias was still evident. These authors
81 attributed the overall improvements in the simulation of sub-daily precipitation to the convection-
82 permitting resolution and improved cloud microphysics. Additionally, two Weather Research and
83 Forecasting model (WRF; Skamarock et al. 2008) experiments over the Tibetan Plateau conducted at
84 'gray-zone' (~9 km) and convection-permitting (~3 km) resolutions for 2009-2018 both showed
85 successful simulation of the spatial pattern and daily variation of surface temperature and precipitation
86 (Ma et al., 2022). Notably, the ability of the convection-permitting WRF RCM in improving
87 precipitation simulation was limited relative to the gray-zone experiment.

88 The sole prior evaluation of reanalysis-driven CORDEX-CMIP5 Australasia regional climate
89 models was conducted by Di Virgilio et al. (2019). This evaluation of CORDEX ERA-Interim forced
90 RCMs focused on four configurations of WRF, and single configurations of CCLM and the
91 Conformal-Cubic Atmospheric Model (CCAM; McGregor and Dix, 2008) to simulate the historical
92 Australian climate (1981–2010) at 50 km resolution. These RCMs showed statistically significant,
93 strong cold biases in maximum temperature, which in some cases exceeded -5 K, contrasting with
94 more accurate simulations of minimum temperature, with biases of ± 1.5 K for most WRF
95 configurations and CCAM. The RCMs generally overestimated precipitation, especially over
96 Australia's highly populated eastern seaboard. Notably, Di Virgilio et al. (2019) observed strong
97 negative correlations between simulated mean monthly biases in precipitation and maximum
98 temperature, suggesting that the maximum temperature cold bias was linked to precipitation
99 overestimation.

100 This study aims to build on that of Di Virgilio et al. (2019) to present the first evaluation of
101 CORDEX-CMIP6 ERA5-forced WRF RCMs over Australia. It has three main aims: 1) to evaluate the
102 capabilities of seven ERA5-forced WRF RCM configurations to simulate the historical Australian
103 climate, assessing the relative strengths and weaknesses of individual RCMs; 2) compare the
104 performance of current generation CORDEX-CMIP6 ERA5 RCMs with the previous generation of
105 CORDEX-CMIP5 ERA-Interim-forced RCMs following the evaluation approach of Di Virgilio et al.
106 (2019); and 3) investigate whether any performance differences observed for the ERA5-forced
107 relative to the ERA-Interim forced RCMs can be attributed to the change in the driving reanalysis data
108 sets or to other factors, such as the use of different RCM physics configurations and model design
109 specifications. Following Di Virgilio et al. (2019) we evaluate the ability of RCMs to simulate near-
110 surface maximum and minimum air temperature and precipitation at annual, seasonal, and daily time
111 scales. Here, our focus is on evaluating the performances of the different RCM generations, with an
112 investigation of the mechanisms underlying the varying model performances to be the subject of
113 future work.

114 **2. Materials and methods**

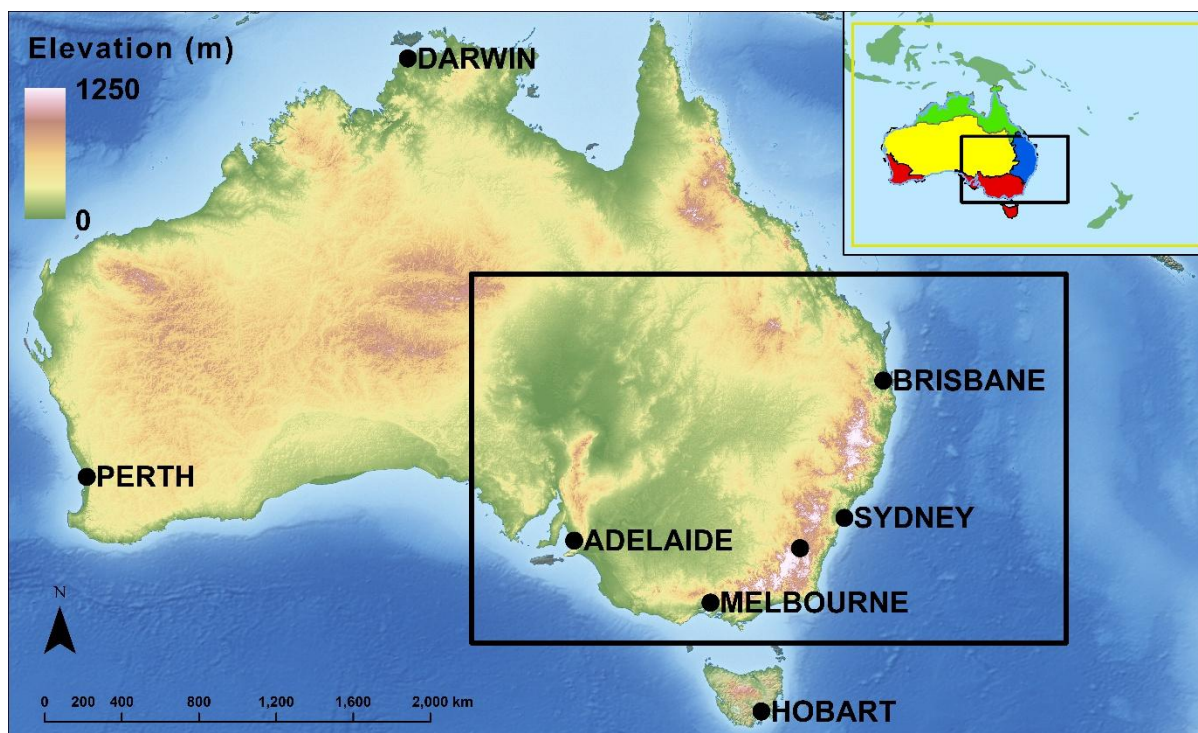
115 **2.1 Models**

116 The CORDEX-CMIP5 ERA-Interim forced RCMs (WRF360J, WRF360K, WRF360L, MU-
117 WRFSWWA, CCAM and CCLM) used a domain with quasi-regular grid spacing of approximately 50
118 km ($0.44^\circ \times 0.44^\circ$ on a rotated coordinate system) over the CORDEX-Australasia region. The ERA-
119 Interim WRF RCMs used different versions of WRF: WRF360J-K-L used WRF version 3.6.0,
120 whereas MU-WRFSWWA used version 3.3. ERA-Interim RCM parameterisations for planetary
121 boundary layer physics, surface physics, cumulus physics, land surface model, and radiation, and
122 vertical level settings are shown in Table 1. Three configurations of CORDEX-CMIP5 ERA-Interim
123 WRF RCMs (WRF360J-K-L) were run using two nested domains with one-way nesting. The inner
124 domain located over south-eastern Australia obtained its initial and lateral boundary conditions from
125 an outer domain simulation located over the CORDEX-Australasia region (Figure 1). The inner
126 domain used a resolution of approximately 10 km. Further details on the ERA-Interim-forced RCMs
127 are provided in Di Virgilio et al. (2019), including overviews of the WRF, CCAM and CCLM RCMs.

128 Seven ERA5-forced RCMs comprise the CORDEX-CMIP6 evaluation experiment for
129 NARcliM2.0 (NSW and Australian Regional Climate Modelling), which is the latest generation of
130 NARcliM simulations (Evans et al., 2014; Nishant et al., 2021) and is one of several RCM ensembles
131 generating dynamically downscaled climate projections for CORDEX-Australasia (Grose et al. 2023).
132 These RCMs were driven by ERA5 boundary conditions for a 42-year period from January 1979 to
133 December 2020. All ERA5 RCMs used WRF version 4.1.2. These CORDEX-CMIP6 ERA5 RCMs

134 were also run using two nested domains with one-way nesting. The outer domain over CORDEX-
135 Australasia used a quasi-regular grid spacing of approximately 20 km ($0.2^\circ \times 0.2^\circ$ on a rotated
136 coordinate system), and the inner domain over south-eastern Australia used a resolution of
137 approximately 4 km. Both domains used 45 vertical levels. The seven WRF RCM configurations (R1-
138 R7) used different parameterisations for planetary boundary layer physics, surface physics, cumulus
139 physics, land surface model (LSM), and radiation, noting that several parameters differed relative to
140 those of the ERA-Interim WRF RCMs (Table 1). Four of the ERA5-RCMs used the Noah-MP LSM
141 with its ‘dynamic vegetation cover’ option activated (referred to as ‘dynamic vegetation’ in the WRF
142 users’ guide) (Niu et al., 2011). When deactivated (the default), monthly leaf area index (LAI) is
143 prescribed for various vegetation types and the greenness vegetation fraction (GVF) comes from
144 monthly GVF climatological values. Conversely, when dynamic vegetation cover is activated, LAI
145 and GVF are calculated using a dynamic leaf model. We clarify here that dominant plant-functional
146 types do not change when using this option, but only the LAI and GVF, i.e. only the amount of green
147 cover changes. Additionally, while the indicated cumulus parametrisation was used in the 20 km-
148 resolution outer domain, all ERA5-forced simulations were made convection-permitting in the 4 km
149 inner domain; i.e. no cumulus parametrisation was used. Urban physics was switched on for these
150 simulations. These two design changes are unique to these ERA5-WRF RCMs.

151 The seven ERA5 WRF configurations were selected from an ensemble of seventy-eight
152 structurally different WRF RCMs. Each of these seventy-eight RCMs used different parameterisations
153 for planetary boundary layer, microphysics, cumulus, radiation, and LSM, where parameterisation
154 options were selected via literature review and recommendations from WRF model developers. These
155 seventy-eight test RCMs were run for an entire annual cycle (2016 with a two-month spin-up period
156 commencing 1 November 2015). The seven ERA5 WRF configurations were selected from this larger
157 ensemble based on their skill in simulating the south-eastern Australian climate, whilst retaining as
158 much independent information as possible (Evans et al. 2014; Di Virgilio et al. 2024). Evaluations of
159 model performances are presented for the Australia landmass only and follow the evaluation method
160 of Di Virgilio et al. (2019) for the same period, i.e. for a 29-year period from January 1981 to January
161 2010. Additionally, select assessments of model performance are presented for the inner domain over
162 south-eastern Australia.



163

164 **Figure 1.** Topographic variation across Australia and major cities Inset: The CORDEX-Australasia
 165 domain and four Natural Resource Management (NRM) regions/climate zones (blue = Eastern
 166 Australia; red = Southern Australia; yellow = Rangelands; and green = Northern Australia). Seven
 167 configurations of CORDEX-CMIP6 ERA5 weather research and forecasting (WRF) RCMs (R1-R7)
 168 and three configurations of CORDEX-CMIP5 ERA-Interim WRF RCMs (WRF360J-K-L) were run
 169 using two nested domains via one-way nesting with an outer domain over CORDEX Australasia and
 170 an inner domain over south-eastern Australia (black rectangle in both main panel and inset).

171 **Table 1.** List of CORDEX-CMIP6 ERA5 and CORDEX-CMIP5 ERA-Interim forced RCMs assessed
 172 by this evaluation study.

Reanalysis	RCM / Version	Planetary boundary layer physics / surface layer physics	Microphysics	Cumulus physics	Shortwave and longwave radiation physics	Land surface	Land options	Vertical Levels
ERA5	R1	YSU (Hong et al., 2006)	WSM6 (Hong and Lim, 2006)	BMJ (Janjić, 2000)	New Goddard (Chou et al., 2001)	Noah Unified (Tewari et al., 2016)	N/A	45
	R2	MYNN2 (Nakanishi and Niino, 2009)	WSM6	Kain-Fritsch (Kain, 2004)	RRTMG (Iacono et al., 2008)	Noah-MP (Niu et al., 2011)	dynamic vegetation	
	R3	MYNN2	Thompson (Thompson et al., 2008)	BMJ	RRTMG	Noah-MP	dynamic vegetation	
	R4	MYNN2	Thompson	BMJ	RRTMG	Noah-MP	TOPMODEL runoff (SIMGM groundwater)	
	R5	ACM2 (Pleim, 2007)	Thompson	BMJ	RRTMG	Noah-MP	dynamic vegetation	
	R6	ACM2	Thompson	Tiedtke (Tiedtke, 1989)	RRTMG	Noah-MP	dynamic vegetation	
	R7	ACM2	Thompson	Tiedtke	RRTMG	Noah-MP	TOPMODEL runoff (SIMGM groundwater)	

	WRF360J	Mellor-Yamada-Janjic/ETA Similarity	WRF Double-Moment 5	Kain-Fritsch	Dudhia/RRTM	Noah Unified	
	WRF360K	Mellor-Yamada-Janjic/ETA Similarity	WRF Double-Moment 5	Betts-Miller-Janjic	Dudhia/RRTM	Noah Unified	
	WRF360L	Yonsei University/MM5 Similarity	WRF Double-Moment 5	Kain-Fritsch	CAM3/CAM3	Noah Unified	30
ERA-I	SWWA WRF330	Yonsei University/MM5 Similarity	WRF Single-Moment 5	Kain-Fritsch	Dudhia/RRTM	Noah Unified	N/A
	CCAM	Monin-Obukhov Similarity Theory stability-dependent boundary-layer scheme (McGregor 1993)	Liquid and ice-water scheme (Rotstayn 1997)	Mass-flux closure (McGregor 2003)	GFDL (Freidenreich and Ramaswamy 1999)	CABLE (Kowalczyk et al. 2006)	27
	CCLM4-8-17-CLM3-5	Prognostic turbulent kinetic energy (Raschendorfer 2001)	Seifert and Beheng (2001), reduced to one moment scheme	Bechtold et al. (2008)	Ritter and Geleyn (1992)	CLM; (Dickinson et al. 2006)	35

173

174 2.2 Observations

175 Australian Gridded Climate Data (AGCD version 1.0; Bureau of Meteorology, 2020; Evans et al., 2020)
 176 were used to evaluate RCM performance. This daily gridded maximum and minimum temperature and
 177 precipitation data set has a grid-averaged resolution of 0.05° and is obtained from an interpolation of
 178 station observations across the Australian continent. Observations include temperature minima and
 179 maxima only; hence, the ability of RCMs to reproduce mean temperature was not assessed. Following
 180 Di Virgilio et al. (2019), the AGCD data were re-gridded to correspond with the RCM data on their
 181 native grids using a conservative area-weighted re-gridding scheme. Most stations used for AGCD are
 182 in coastal areas, contrasting with a sparser representation inland, and especially in Australia's north-
 183 west. There are more precipitation stations than temperature stations. Only land points over Australia
 184 were evaluated because AGCD observations are terrestrial data.

185 2.3 Evaluation methods

186 2.3.1 Evaluations of CORDEX-CMIP6 ERA5 RCMs versus CORDEX-CMIP5 ERA- 187 Interim RCMs

188 Annual and seasonal means were calculated for maximum and minimum temperature and precipitation
 189 using monthly averages for each temperature variable, and the monthly sum for precipitation.
 190 Percentiles (i.e. extremes: 99th percentiles for maximum temperature and precipitation; 1st percentile for
 191 minimum temperature) were calculated using daily values. RCM performances in reproducing
 192 observations over these timescales were assessed by calculating the model bias, i.e. model outputs
 193 minus observations, and the RMSE of modelled versus observed fields. The statistical significance of
 194 mean annual and seasonal biases compared to the AGCD observations was calculated for each grid cell
 195 using t-tests ($\alpha = 0.05$) for maximum and minimum temperature assuming equal variance. The Mann-
 196 Whitney U test was used for precipitation given its non-normality. Results on the statistical significance

197 of each ensemble mean were separated into three categories following Tebaldi et al. (2011): 1)
198 statistically insignificant areas are shown in colour, denoting that less than 50% of RCMs are
199 significantly biased, which is the most desired outcome; 2) in areas of significant agreement (stippled),
200 at least 50% of RCMs are significantly biased and at least 66% of significant models agree on the sign
201 of the bias. In such areas, many ensemble members have the same bias sign which is an undesirable
202 outcome; and 3) areas of significant disagreement are shown in white, where at least 50% of RCMs are
203 significantly biased and fewer than 66% of significant models agree on the bias sign.

204 The ability of the RCMs to simulate observed variables at daily time scales was also assessed
205 by comparing the probability density functions (PDFs) for daily mean observations versus those of the
206 RCMs. PDFs were separately calculated for Australia and for each of four natural resource management
207 (NRM) climate regions shown in Figure 1 for maximum and minimum temperature, and precipitation.
208 Here, daily precipitation values below 0.1 mm were omitted from the RCM output, because rates below
209 this amount fall below the detection limit of the stations used to produce the observed data set.
210 Additionally, the daily rainfall observational network used to produce the AGCD has large gaps in
211 several areas of central Australia; hence, RCM output was masked over these areas. RCM and observed
212 PDFs were compared using the Perkins Skill Score (PSS; Perkins et al. (2007), which measures the
213 degree of overlap between two PDFs, with PSS = 1 indicating that the distributions overlap perfectly.

214 ***2.3.2 Comparing ERA5 versus ERA-Interim RCM performances after switching driving*** 215 ***reanalyses***

216 Any performance differences of the ERA5-forced and ERA-Interim-forced RCMs could be partially
217 due to the change in the driving reanalysis, as well as factors such as different RCM physics
218 configurations, model version and other design specifications. To assess whether the change in ERA5
219 versus ERA-Interim driving reanalyses may underlie differences in performance profiles of the WRF
220 RCMs from the two generations of CORDEX experiment we conduct two investigations: 1) the ERA5
221 and ERA-Interim reanalysis data are compared against AGCD observations to assess their degree of
222 bias for annual and seasonal timescales; and 2) fourteen-month simulations are performed where
223 otherwise identically parameterised and configured CORDEX-CMIP6 NARClM2.0 R1-R7 RCMs are
224 forced by ERA-Interim as opposed to ERA5, and similarly the WRFJ-K-L RCMs from the CORDEX-
225 CMIP5 era are forced with ERA5 instead of ERA-Interim. For instance, the ERA5-RCMs CORDEX-
226 CMIP6 (NARClM2.0) RCMs are run for the same 4 km convection permitting domain using the same
227 physics options and model setups with the only changes being to swap ERA5 for ERA-Interim and
228 running for 14 months. These simulations start on 1 November 2015, with evaluation performed for the
229 twelve months of 2016, i.e. using the first 2-months as spin-up period. Australia experienced a range of
230 weather extremes during 2016 driven by a range of climatic influences making 2016 a suitable target
231 year (Bureau of Meteorology, 2017). Owing to finite compute resources, it was not possible to simulate
232 for a longer period for these experiments.

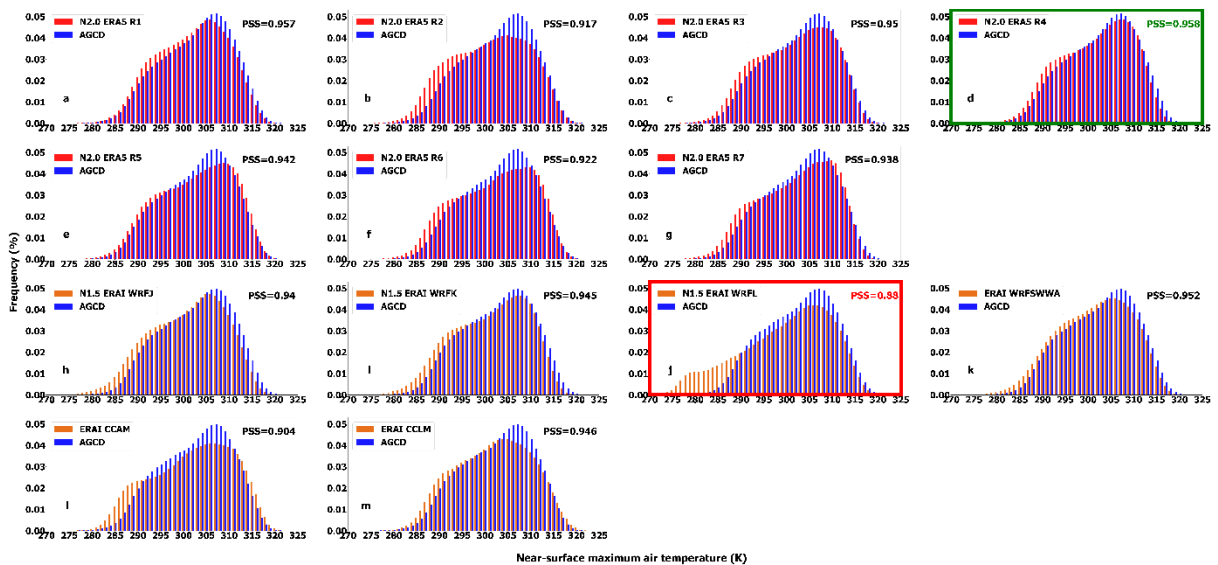
233 3. Results

234 RCM evaluation results are presented first for the 29-year CORDEX-CMIP6 ERA5-forced and
 235 CORDEX-CMIP5 ERA-Interim-forced simulations. Evaluation results from switching the driving
 236 reanalyses of the CORDEX-CMIP6 and CORDEX-CMIP5 RCMs are then considered.

237 3.1 Evaluation of CORDEX-CMIP6 ERA5-RCM and CORDEX-CMIP5 238 ERA-Interim performances

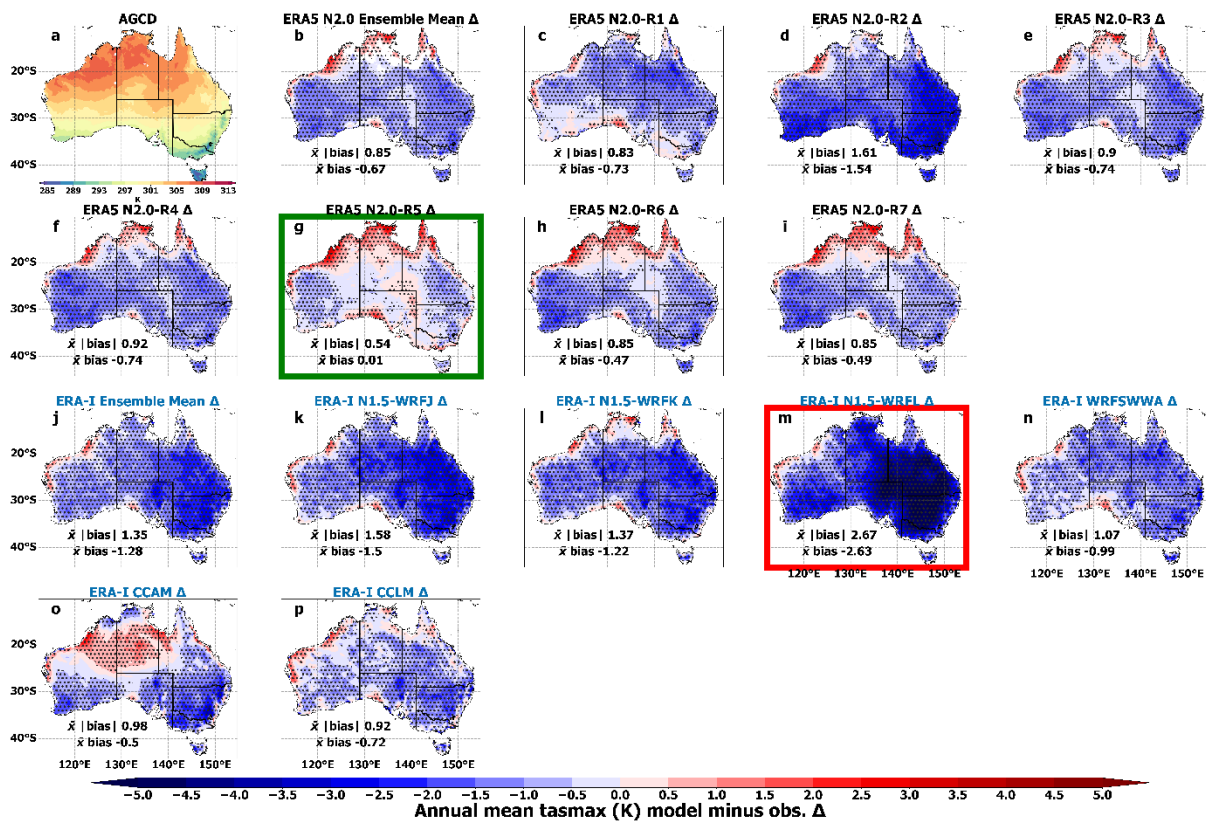
239 3.1.1 Maximum Temperature

240 Both ERA5 and ERA-Interim forced RCMs overestimate the frequency of lower-than-average
 241 maximum temperatures and underestimate the observed peaks (Fig. 2). However, most ERA5 RCMs
 242 simulate occurrences of warmer than average temperatures more accurately than the ERA-Interim
 243 RCMs, especially ERA5-R3 (Fig. 2c). The ERA5-RCMs with highest PSS scores (i.e. >0.95; R1 and
 244 R4) show closer correspondences to the observed peaks than the other ERA5-RCMs, but they
 245 underestimate the distribution right tail. In some respects, RCM performances in PDFs stratified by
 246 NRM region can show different patterns of results versus the nationally aggregated data (Online
 247 Resource 1: Figures S1-S4). For instance, most ERA5-RCMs show larger over-estimations of warmer
 248 than average daily maximum temperatures over the Northern Australia region (Figure S4) than for
 249 Australia-wide data (Figure 2).



250
 251 **Figure 2.** Probability density functions (PDFs) of mean daily maximum near-surface air temperatures
 252 (K) across Australia for 1981-2010. Panels a-m show the PDF of a specific RCM configuration
 253 relative to that of Australian Gridded Climate Data (AGCD) observations; a-g are NARClIM2.0
 254 ERA5-forced RCM configurations; h-m are ERA-Interim-forced RCM configurations. Panel
 255 boundaries in green (red) indicate the RCMs with highest (lowest) PSS. PDF bin width is 1 K.

256 Most ERA5-RCMs show small cold biases of ~ 0.5 to 1 K for annual mean maximum
 257 temperature over most of Australia, except for warm biases of ~ 0.5 to 1.5 K over the coastal north,
 258 depending on location/RCM configuration (Fig. 3 b-i). ERA5-R5-R7 show lowest area-averaged
 259 absolute annual biases, with R5 showing very small biases of < 0.5 K over much of eastern Australia
 260 (Fig. 3g). ERA5-R2 shows markedly poorer performance than every other ERA5 RCM, with cold
 261 biases exceeding 2 K in some areas (Fig. 3d). The positive biases of maximum temperature over the
 262 tropics for several of the ERA5-RCMs generally correspond well to negative precipitation biases over
 263 this region (see Fig. 7b; e-i). Except for ERA5-R2, the ERA5-forced RCMs show considerable
 264 reductions in the magnitude of cold bias relative to the ERA-Interim forced RCMs (Fig.3 j-p). The
 265 best-performing ERA5-RCM (R5) has an area-averaged absolute mean bias of 0.54 K, as compared to
 266 0.92 K for the best performing ERA-Interim RCM (CCLM), a 52% percentage difference. ERA5-R5
 267 has a 66% percentage difference in absolute bias compared to the best performing ERA-Interim WRF
 268 RCM (i.e. WRFSSWA: 1.07 K).



269

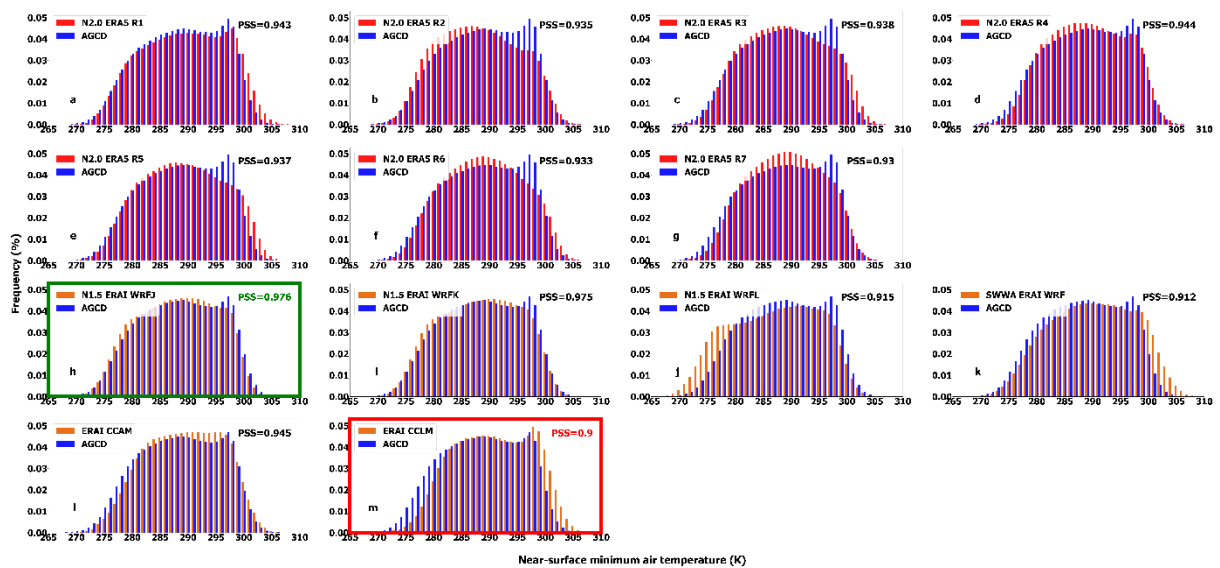
270 **Figure 3.** Annual mean near-surface atmospheric maximum temperature bias with respect to
 271 Australian Gridded Climate Data (AGCD) observations for 1981-2010. Stippled areas indicate
 272 locations where an RCM shows statistically significant bias ($P < 0.05$). b Significance stippling for
 273 the ensemble mean bias follows Tebaldi et al. (2011) and is applied separately to each of the two
 274 RCM ensembles. Statistically insignificant areas are shown in colour, denoting that less than half of
 275 the models are significantly biased. In significant agreeing areas (stippled), at least half of RCMs are
 276 significantly biased, and at least 66% of significant RCMs in each ensemble agree on the direction of
 277 the bias. Significant disagreeing areas are shown in white, which are where at least half of the models
 278 are significantly biased and less than 66% of significant models in each ensemble agree on the bias
 279 direction - see main text for additional detail on the stippling regime. Panel boundaries in green (red)
 280 indicate the RCMs with lowest (highest) area-averaged mean absolute biases

281 During summer, the magnitude and spatial extent of maximum temperature warm biases
 282 increase for all RCMs relative to the annual mean biases (Fig. S5). During winter, several ERA5
 283 RCMs (R1, R3, R4, R5) retain much smaller cold biases than most ERA-Interim-forced models (Fig.
 284 S6). RMSE magnitudes peak for most ERA5 and ERA-Interim models in February (at the end of
 285 austral summer), except for several ERA-Interim RCMs which show larger RMSEs in winter,
 286 especially ERAI-WRFL; Fig. S7).

287 For extreme (99th percentile) maximum temperatures, whilst ERA5-RCMs show lower overall
 288 biases relative to the ERA-Interim RCMs, the former show strong warm biases along coastlines that
 289 are typically stronger than biases further inland (Fig. S8). These biases are particularly pronounced
 290 along northern and eastern coastlines. ERA5-R1 and R5 show the lowest overall mean absolute biases
 291 for extreme maximum temperature, especially over south-eastern Australia. The various mean
 292 absolute bias and PSS statistics for maximum temperature for the 20 km domain are summarised in
 293 Online Resource Table S1.

294 3.1.2 Minimum Temperature

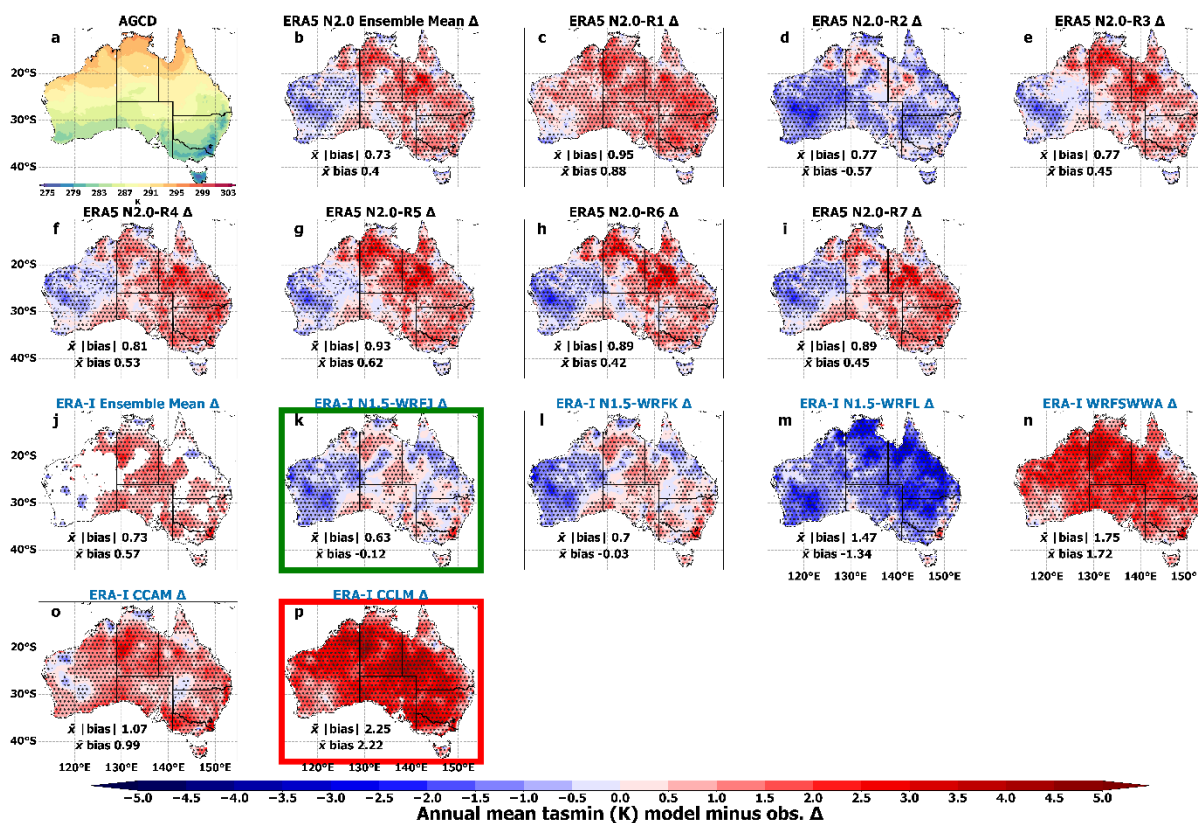
295 PDFs of daily minimum temperature for the ERA-Interim-forced WRFJ and WRFK RCMs match
 296 observations most closely relative to the ERA5- and other ERA-Interim forced RCMs (Fig. 4).
 297 Observed PDFs at the continental scale show a slight bimodality that is captured by ERA5-R1, ERA5-
 298 R4, ERAI-WFJ, ERAI-SWWA and ERAI-CCLM. However, this bimodality is generally not present
 299 in PDFs stratified for specific NRM regions (Figures S9-S12). Several RCMs struggle to simulate
 300 minimum temperature occurrences in the middle of the distribution (i.e. ~285-290K), except for
 301 ERA5-R5 and ERA-Interim-WRFJ, WRFK, and CCLM which closely match minimum temperatures
 302 in this range.



303
 304 **Figure 4.** Probability density functions (PDFs) of mean daily minimum near-surface air temperatures
 305 (K) across Australia for 1981-2010. Panels a-m show the PDF of a specific RCM configuration
 306 relative to that of Australian Gridded Climate Data (AGCD) observations; a-g are NARClm2.0

307 ERA5-forced RCM configurations; h-m are ERA-Interim-forced RCM configurations. Panel
 308 boundary colouring as per Fig. 2. PDF bin width is 1 K.

309 ERA5-RCMs generally overestimate mean minimum temperature annually (Fig. 5) and
 310 seasonally (Fig S13-summer and S14-winter), except for ERA5-R2 which is cold biased. In contrast,
 311 ERA-Interim-RCMs show a mixed signal for WRF-J and WRF-K, cold bias for WRF-L and warm
 312 biases for the remaining RCMs. Warm biases are strongest during JJA for most ERA5-RCMs, and
 313 especially for ERA-Interim CCAM and CCLM (Fig. S14). Whereas ERA5-R2 performs generally
 314 poorly for maximum temperature relative to the other ERA5-RCMs (e.g. annual mean absolute bias =
 315 1.61K), its bias is substantially reduced for minimum temperature (annual mean absolute bias =
 316 0.77K). ERA5 R2 and R3 show better performance for minimum temperature relative to the other
 317 ERA5-RCMs. Their area-averaged annual mean absolute biases (0.77K in both cases) are more
 318 comparable to the ERA-Interim-forced WRFJ-K RCMs which simulate annual mean minimum
 319 temperature most accurately (annual mean absolute biases = 0.66K and 0.7 K, respectively).



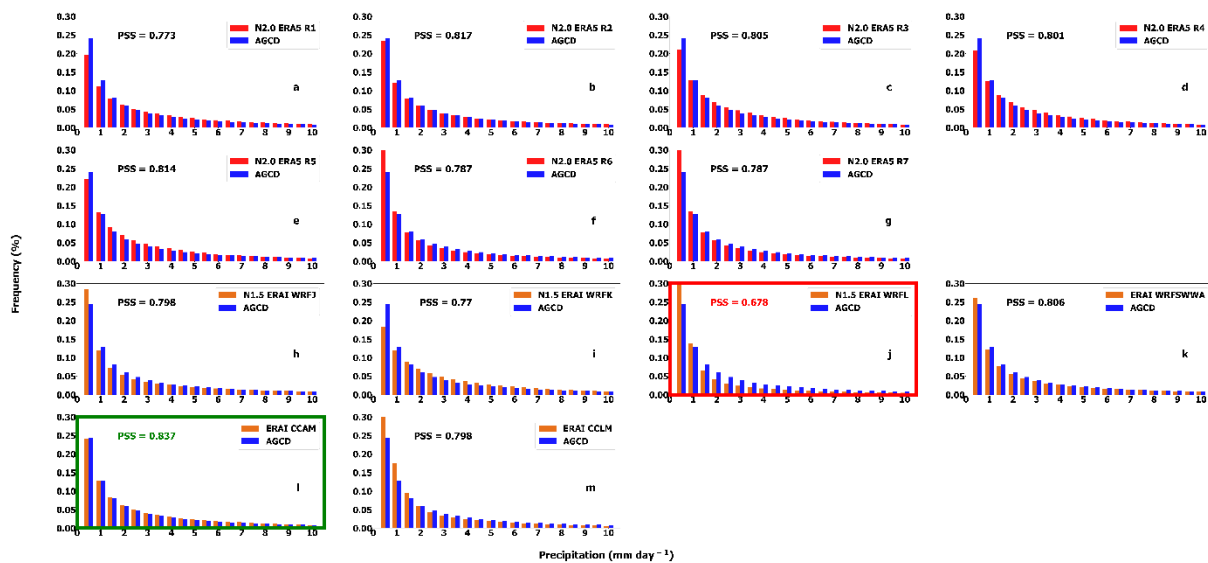
320
 321 **Figure 5.** Annual mean near-surface atmospheric minimum temperature bias with respect to gridded
 322 observations for 1981-2010. Stippling and panel boundary colouring as per Fig. 3

323 RMSE annual cycles for mean minimum temperature broadly reflect the above pattern of
 324 results (Fig. S15). For most months throughout the annual cycle, RMSEs are typically lowest for
 325 ERA-Interim WRFJ-K. However, ERA5-R1, R2 also show small RMSEs from May to August, with
 326 RMSEs also being low for ERA5-R3 during spring (September to November).

327 The majority of ERA5 and ERA-Interim RCMs are generally warm-biased for extreme
 328 minimum temperature over most of Australia, with only small areas of cold bias over the north-west
 329 (Fig. S16). The exceptions are ERA5-R2 and ERA-Interim-WRFJ-K which show biases of mixed sign
 330 across larger areas of Australia, and ERA-Interim WRFL which is strongly cold biased (Fig. S16).
 331 ERA5-R2 and R3 show reasonably good performance for extreme minimum temperature as compared
 332 to the other ERA5 models, however, ERA-Interim WRFJ-K simulate extreme minimum temperature
 333 most accurately. Mean absolute bias and PSS statistics for minimum temperature for the 20 km
 334 domain are summarised in Table S1.

335 3.1.3 Precipitation

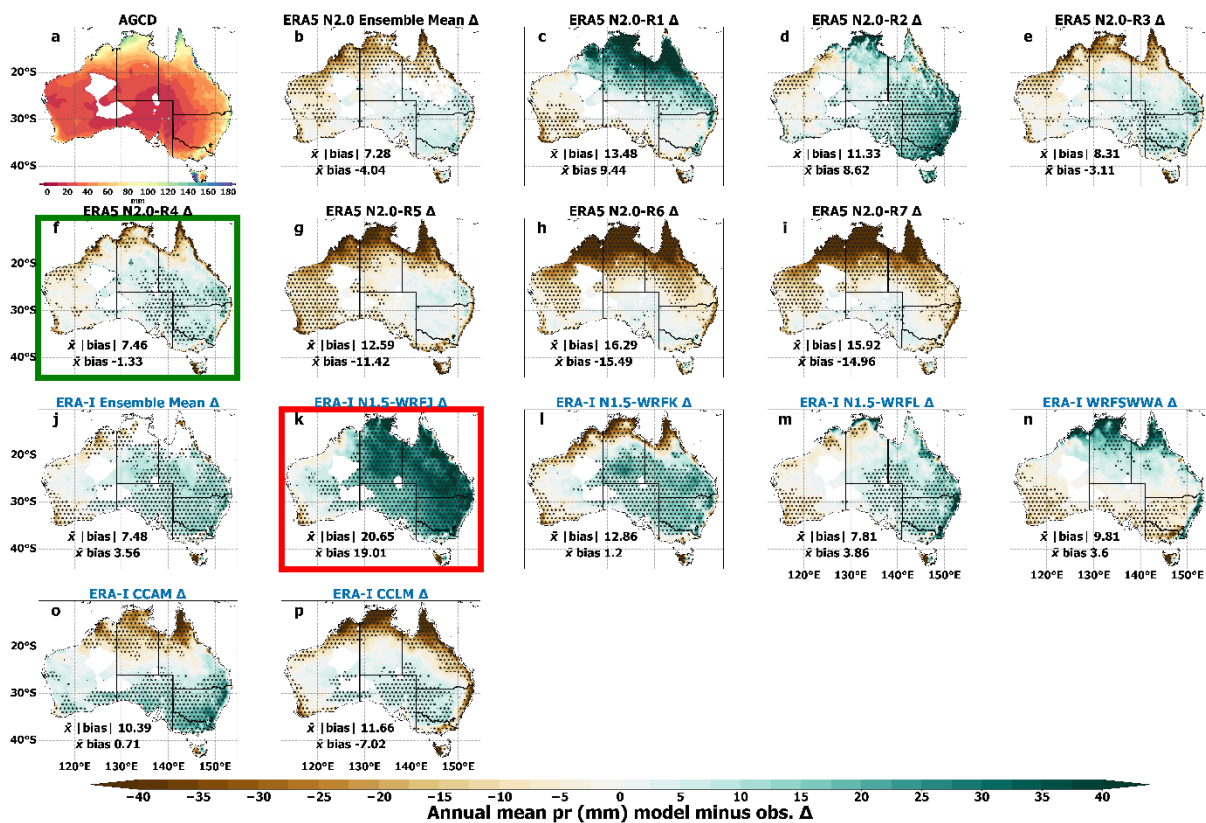
336 PDFs of mean daily precipitation show that ERA5-R2, ERA-Interim-forced CCAM and WRFSWWA
 337 simulate the occurrence of rainfall events up to 5 mm day⁻¹ more accurately than the other RCMs (Fig.
 338 6). Heavier rainfall events (approximately >7 mm day⁻¹) are underestimated by several RCMs.
 339 Overall, the ERA5-RCMs simulate daily precipitation occurrences consistently better than the ERA-
 340 Interim-RCMs, i.e. four of the seven ERA5-RCMs have PSS >0.8 compared to two of six ERA-
 341 Interim RCMs. Of the ERA5-forced RCMs, R2 produces the best simulation of daily rainfall
 342 occurrences. There are some interesting differences in RCM performance between the NRM regions
 343 (Fig. S17-S20). For instance, most RCMs generally show more skill in capturing daily precipitation
 344 distributions over Southern Australia than other NRM regions, with the ERA5-RCMs performing
 345 particularly well over this region (Fig. S18). Conversely, performances of most RCMs are generally
 346 poorer over Northern Australia than other regions, though ERA5-R5 and ERA-Interim-CCAM show
 347 better performances than their peers over this region with PSS of 0.743 and 0.746, respectively, versus
 348 mean PSS of 0.697 (standard deviation = 0.058; Fig. S20).



349
 350 **Figure 6.** Probability density functions (PDFs) of mean daily precipitation (mm day⁻¹) across
 351 Australia for 1981-2010. Panels a-m show the PDF of a specific RCM configuration relative to that of
 352 Australian Gridded Climate Data (AGCD) observations; a-g are NARClIM2.0 ERA5-forced RCM

353 configurations; h-m are ERA-Interim-forced RCM configurations. Panel boundary colouring as per
 354 Fig. 2. PDF bin width is 0.5 mm.

355 All ERA5 RCMs except for R1 and R2 are dry-biased for annual mean precipitation over the
 356 monsoonal north (Fig. 7), with R6-7 producing the strongest dry biases exceeding -40 mm over this
 357 region (Fig. 7h-i). Of the ERA5 RCMs, R1 and R2 are exceptional in that they show widespread wet
 358 biases. ERA5-R1 and R2 both use WSM6 microphysics, whereas R3-R7 use Thompson microphysics
 359 (see Discussion 4.1). ERA5-R2 shows the strongest wet-bias over eastern Australia of ~20 mm,
 360 whereas ERA5-R3-4 show smaller wet biases (~5-10 mm) over this region. All ERA5-forced models
 361 show dry biases (between -20 and -35 mm) along the south-western coastline of western Australia.
 362 Overall, with the exceptions of R6 and R7, the ERA5-forced RCMs show reduced mean precipitation
 363 bias relative to the ERA-Interim forced RCMs, especially over southeastern Australia. All RCMs
 364 show the strongest biases (of either sign) during DJF (Fig. S21). For instance, the area and magnitude
 365 of dry-bias over northern Australia increase for ERA5-R3-R7 (Fig. S21). All RCMs show the smallest
 366 biases during JJA (Fig. S22).



367
 368 **Figure 7.** Annual mean precipitation bias with respect to gridded observations for the RCMs for
 369 1981-2010. Stippling and panel boundary colouring as per Fig. 3.

370 Overall, RMSE annual cycles are similar for the different RCMs (Fig. S23). ERA-Interim
 371 CCAM has the lowest RMSEs throughout the year. Otherwise, all ERA5-forced RCMs have lower
 372 RMSEs than the ERA-Interim forced models (except for CCAM) from April to October, which is an
 373 important growing season in southern Australia.

374 The ERA5-RCMs generally over-estimate extreme precipitation over Australia and especially
375 the south-east, though R3, R4 and R5 show widespread dry biases over north-western regions (Fig.
376 S24). The R1 and R2 RCMs show larger extreme precipitation wet biases relative to the other ERA5
377 RCMs (i.e. mean absolute biases of 20.02 mm and 14.83 mm, versus 9.21 mm to 11.4 mm, Fig. S24).
378 Several ERA-Interim-forced RCMs (i.e. WRFJ, WRFK, WRFL) produce similar patterns of bias to
379 the ERA5 RCMs, for instance, with wet biases over south-eastern Australia and dry biases over
380 northern and central regions. Overall, the magnitude of biases over the outer domains is similar
381 between the different RCM generations, with several RCMs showing low mean absolute biases
382 ranging from 8.75 mm to 10.25 mm. However, focusing specifically on the high-resolution inner
383 domains of ERA5-RCMs and ERA-Interim-WRFJ-K-L RCMs, noting this domain is uniquely
384 convection-permitting (~4 km) for ERA5-RCMs, most ERA5-RCMs show smaller biases than WRFJ-
385 K-L (Fig. S25). For this inner domain, ERA5-R3, R5, R6, R7 show small biases (i.e. <9 mm),
386 particularly over south-eastern coastal areas. Mean absolute bias and PSS statistics for precipitation
387 for the 20 km domain are summarised in Table S1.

388 **3.2 Assessing the effects of switching driving ERA5 versus ERA-Interim** 389 **reanalyses on RCM performances**

390 This section investigates whether performance differences of the ERA5-forced and ERA-Interim-
391 forced RCMs may be attributable to the different generations of driving reanalyses as opposed to
392 factors such as different RCM physics parameterisations and design specifications. First, biases in the
393 two reanalyses data sets with respect to observations are assessed. The assessment then focuses on the
394 capacities of the CORDEX-CMIP6 era R1-R7 RCMs and the CORDEX-CMIP5 era WRFJ-K-L
395 RCMs to simulate the south-eastern Australian climate when each RCM generation uses first ERA5
396 and then ERA-Interim driving data. This assessment also provides a further view of the how the WRF
397 RCM performances vary over this high-resolution domain relative to the CORDEX Australasia
398 domain. These comparative simulations are only available for the higher resolution inner domain over
399 south-eastern Australia.

400 ***3.2.1 ERA5 and ERA-Interim reanalysis biases relative to observations***

401 Both ERA5 and ERA-Interim are generally cold biased in their simulation of mean maximum
402 temperature at annual, summer and winter timescales during 1981-2010 (Fig. S26). However, biases
403 are larger in magnitude for ERA-Interim relative to ERA5, especially during summer i.e. ERA5 mean
404 absolute bias = 1.22 K; ERA-Interim = 2.07 K. Biases in ERA5 and ERA-Interim during 2016 are
405 largely consistent with these results (Fig. S27).

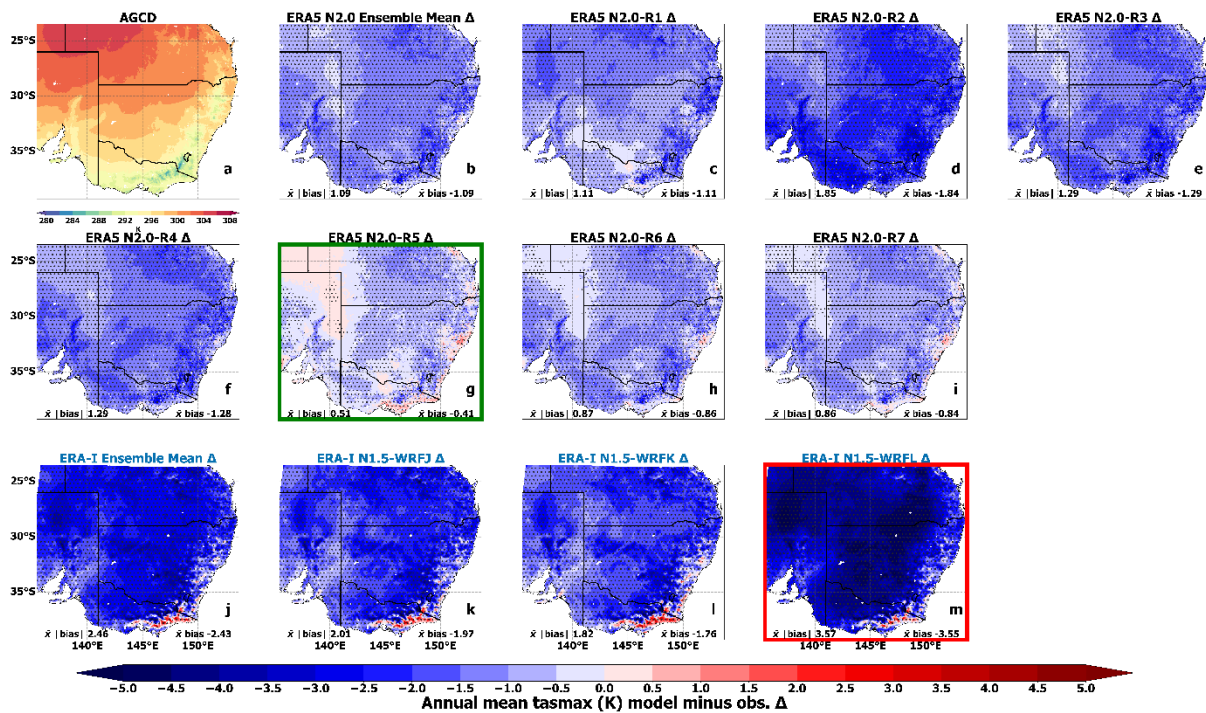
406 ERA5 and ERA-Interim overestimate mean minimum temperature over most of Australia at
407 all timescales for both 1981-2010 (Fig. S28) and 2016 (Fig. S29). Biases are again smaller for ERA5

408 than for ERA-Interim. For ERA-Interim, warm biases are especially large in magnitude along the
 409 eastern and southern coastlines and over the island of Tasmania.

410 ERA5 shows substantial improvements in simulating mean precipitation at all timescales
 411 relative to ERA-Interim (Fig. S30, i.e. ERA5 annal mean absolute bias = 4.18 mm; ERA-Interim =
 412 8.14 mm). This applies to both periods assessed, i.e. including for 2016 (Fig. S31). Additional
 413 differences in the biases between the reanalysis data sets include ERA-Interim's stronger dry biases
 414 over the monsoonal north during summer (wet season) and marked dry biases along the eastern
 415 coastline and elevated terrain in south-eastern Australia (Fig. S30).

416 3.2.2 Comparing RCM performances after switching the driving reanalyses

417 Prior to switching the driving reanalyses of the two generations of RCMs, the ERA5-NARClIM2.0
 418 RCMs show large reductions in cold bias (Fig. 8b-i) relative to the ERA-Interim-forced RCMs (Fig.
 419 8j-m), with ensemble mean bias magnitudes of 1.09K and 2.46K, respectively.

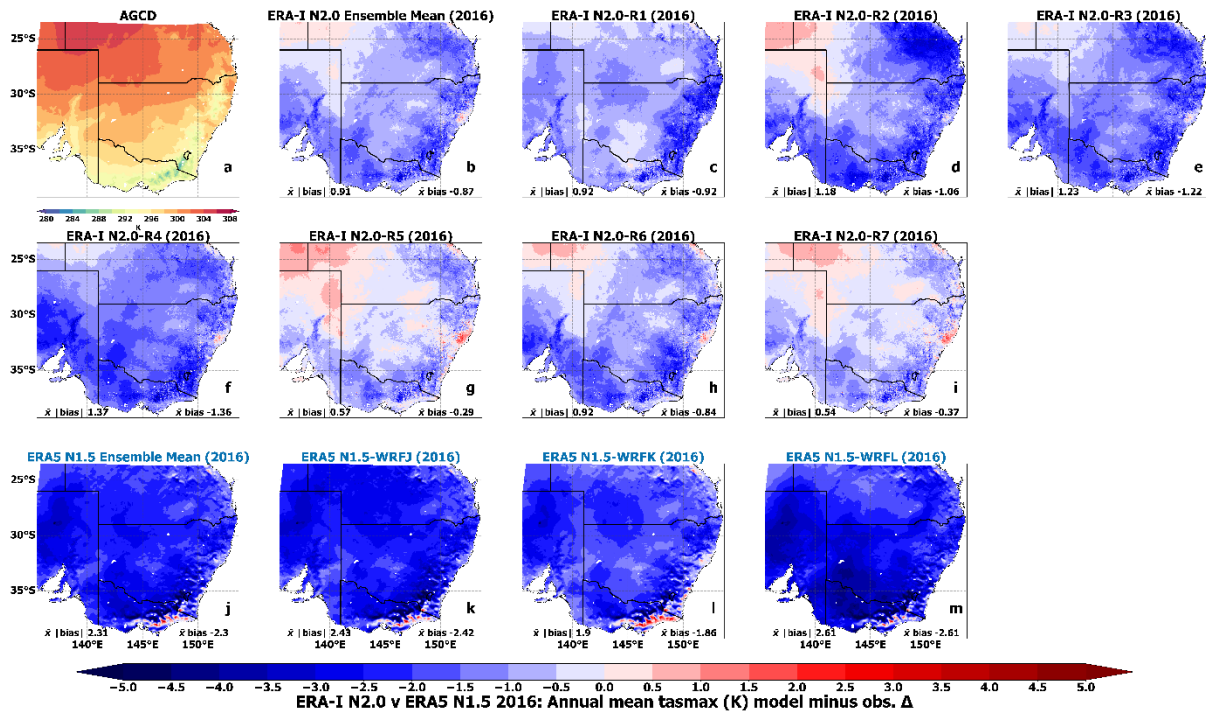


420

421 **Figure 8.** Annual mean near-surface atmospheric maximum temperature bias simulated over south-
 422 eastern Australia (WRF simulation inner domain) with respect to gridded observations for the period
 423 1981-2010 for NARClIM2.0 RCMs (b-i) and NARClIM1.5 RCMs (j-m). Stippling and panel
 424 boundary colouring as per Fig. 3.

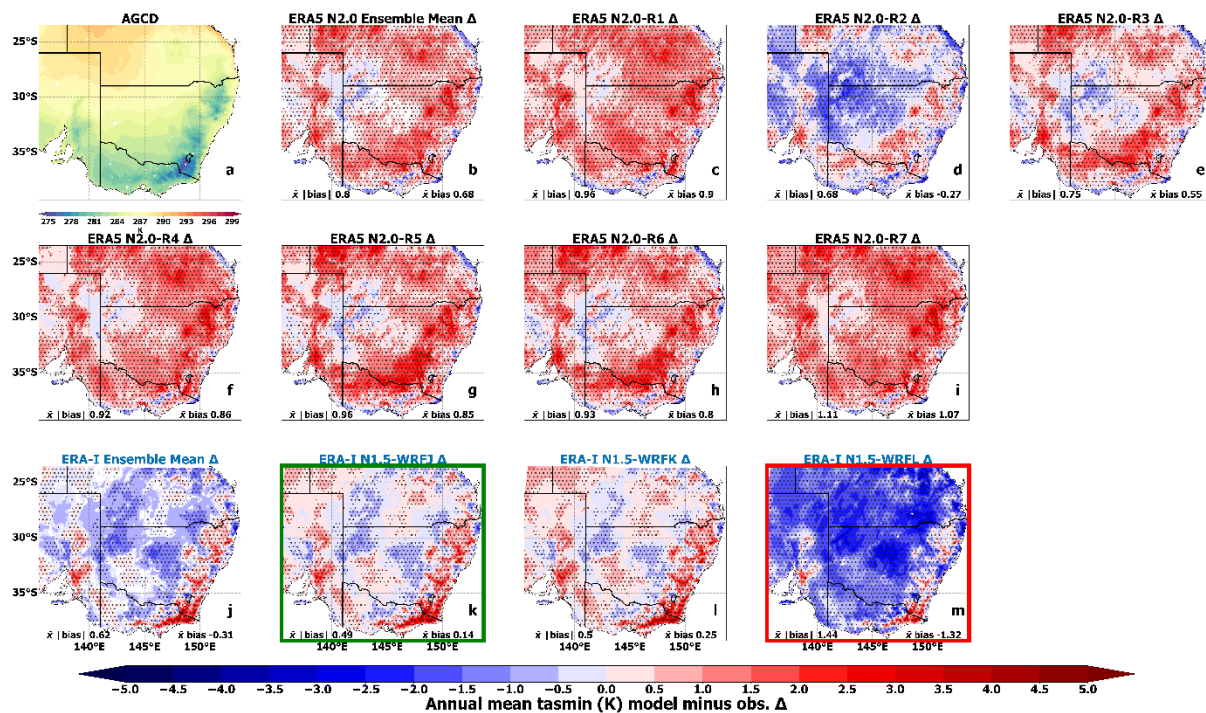
425 Switching the driving reanalysis of the CORDEX-CMIP6 NARClIM2.0 RCMs shows small
 426 improvements in the simulation of maximum temperature for several ERA-Interim-forced
 427 NARClIM2.0 RCMs (i.e. for R1, R2, R3 and R7; Fig. 9c,d,e,i). In contrast, ERA-Interim-
 428 NARClIM2.0 R4-5-6 show slight degradations in performance (Fig. 9f,g,h). However, the
 429 NARClIM2.0 ERA-Interim ensemble mean average absolute bias is 0.91K versus 1.09K for the
 430 NARClIM2.0 ERA5 ensemble. Therefore, overall, there is a small performance improvement in

431 forcing the CORDEX-CMIP6 era RCMs using the older reanalysis. Similarly, the CORDEX-CMIP5
 432 era WRFJ and WRFK show poorer simulations of maximum temperature when forced using ERA5
 433 (Fig. 9k-l) relative to their ERA-Interim-forced counterparts, with only ERA5-WRFL showing a
 434 marked improvement (Fig. 9m).



435
 436 **Figure 9.** Annual mean near-surface atmospheric maximum temperature bias simulated over south-
 437 eastern Australia (WRF simulation inner domain) with respect to gridded observations for
 438 NARClM2.0 RCMs forced by ERA-Interim for 2016 plus two months spin-up starting in November
 439 2015 (a-i), and corresponding NARClM1.5 simulations for the same period forced by ERA5 (j-m).

440 In terms of RCM performances in simulating minimum temperature prior to switching the
 441 driving reanalyses, ERA-Interim-forced WRFJ-K-L RCMs of the CORDEX-CMIP5 era have lower
 442 overall biases for minimum temperature over the inner domain relative to the NARClM2.0 ERA5-
 443 R1-R7 RCMs (i.e. ensemble mean absolute biases are 0.62K and 0.8K, respectively; Fig. 10b,j).
 444 However, the biases of each RCM generation vary geographically, such that the bias magnitudes for
 445 some ERA5-RCMs (e.g. R2-R3) are lower along coastal areas relative to ERA-Interim WRFJ-K-L
 446 over the same areas (Fig. 10d-e; k-m). Conversely, biases are lower over inland regions for ERA-
 447 Interim WRFJ-K-L relative to ERA5-RCMs.

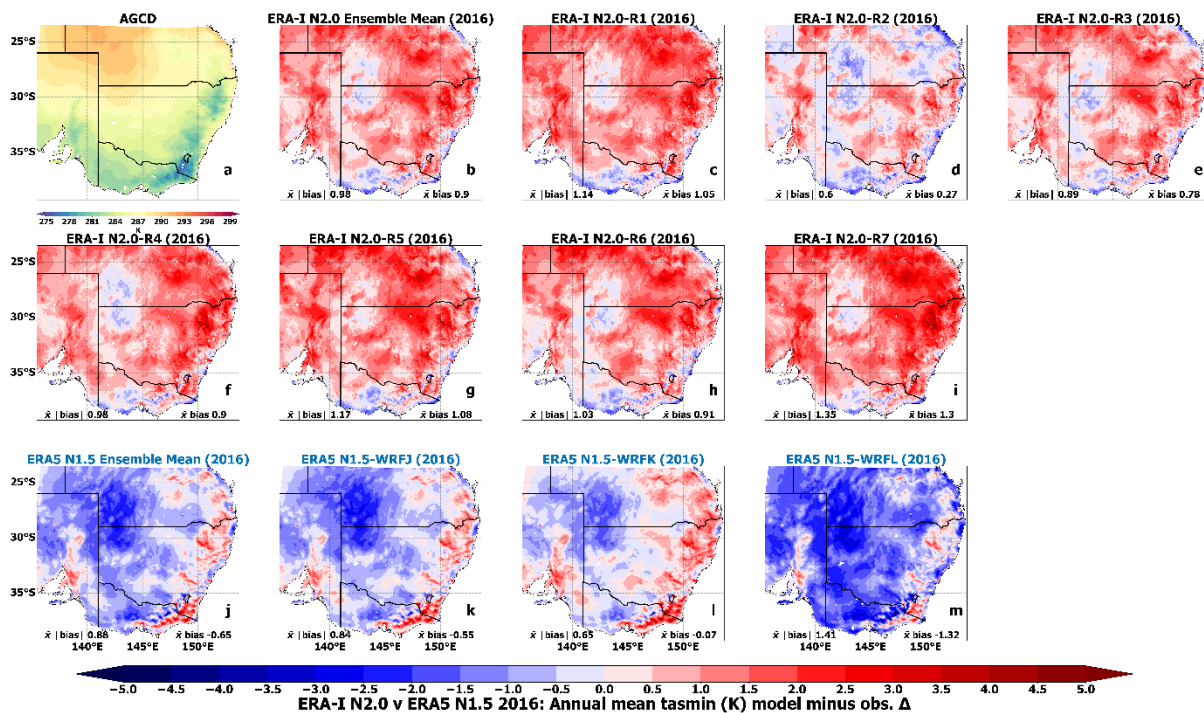


448

449 **Figure 10.** Annual mean near-surface atmospheric minimum temperature bias simulated over south-
 450 eastern Australia (WRF simulation inner domain) with respect to gridded observations for the period
 451 1981-2010 for NARcliM2.0 RCMs (b-i) and NARcliM1.5 RCMs (j-m). Stippling and panel
 452 boundary colouring as per Fig. 3.

453

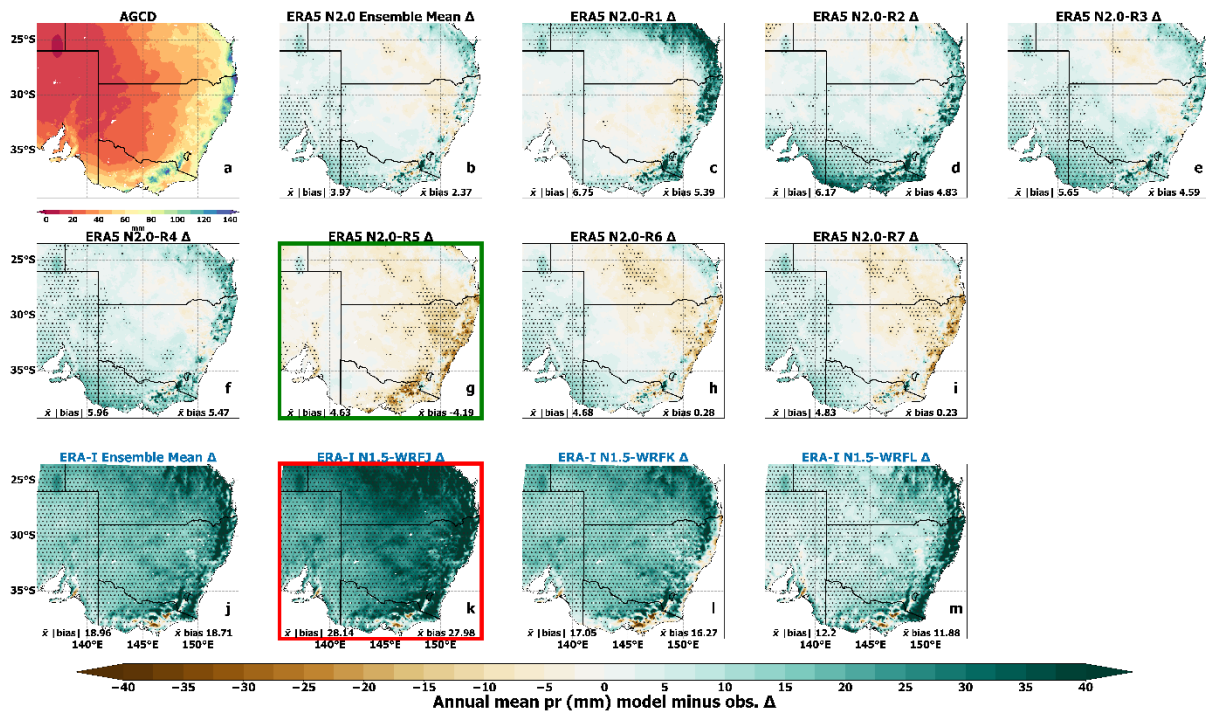
454 Considering RCM simulations of mean minimum temperature with the driving reanalyses
 455 switched, performances are typically substantially poorer for the ERA5-forced WRFJ-K-L RCMs
 456 (Fig. 11) relative to their ERA-Interim-forced counterparts: the ensemble mean absolute biases are
 457 0.88K versus 0.62K, respectively. In contrast, although all NARcliM2.0 RCMs except R2 show
 458 performance degradations when forced with ERA-Interim instead of ERA5 (e.g. ensemble mean
 biases are 0.98K and 0.8K, respectively), these deteriorations are small (Fig. 11b-i).



459

460 **Figure 11.** Annual mean near-surface atmospheric minimum temperature bias with respect to gridded
 461 observations for NARClM2.0 RCMs forced by ERA-Interim for 2016 plus two months spin-up
 462 starting in November 2015 (a-i), and corresponding NARClM1.5 simulations for the same period
 463 forced by ERA5 (j-m).

464 Improvements in the simulation of mean precipitation for ERA5-forced R1-R7 RCMs versus
 465 ERA-Interim WRFJ-K-L RCMs are especially evident over the high resolution south-eastern inner
 466 domain. At this scale, biases for several ERA5-forced R1-R7 RCMs are $< \sim 5$ mm compared to $> \sim 15$
 467 mm for the ERA-Interim-WRFJ-K-L RCMs (Fig. 12). Moreover, several improvements in the ERA5-
 468 RCM simulation of annual mean precipitation are apparent at convection permitting scale relative to
 469 over the 20 km outer domain. For instance, dry biases for ERA5-R3 and R5 along the eastern
 470 coastline are reduced at the convection-permitting scale.

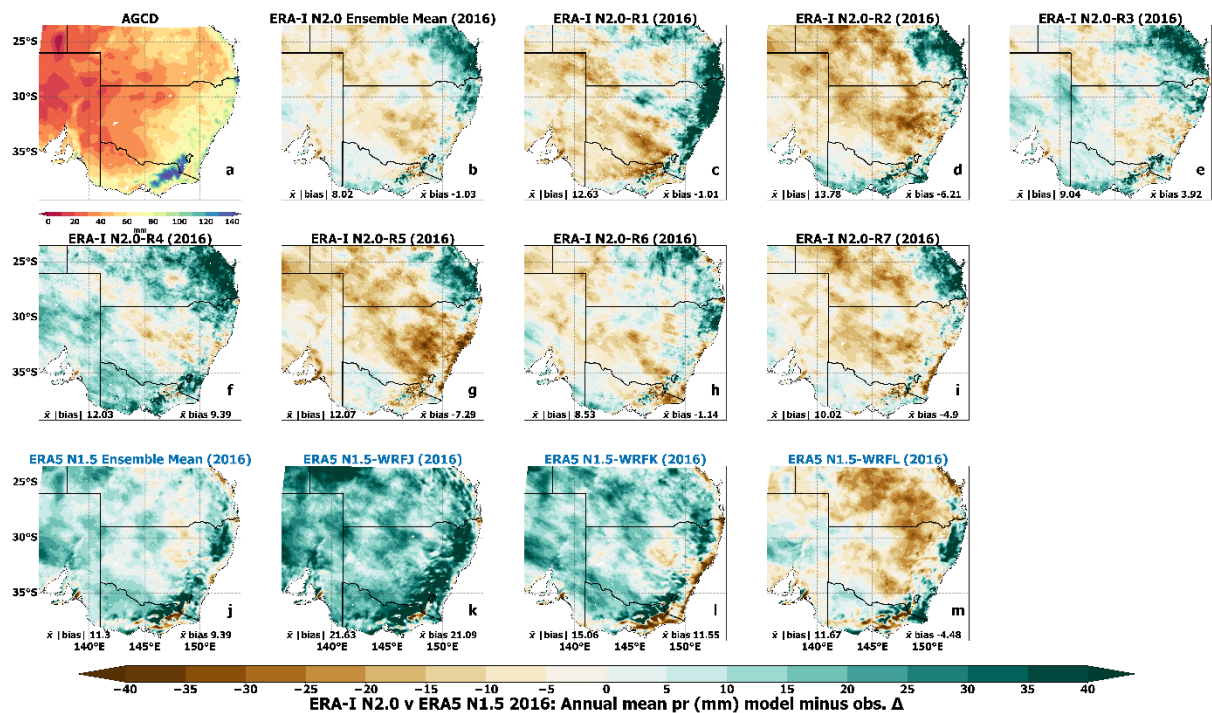


471

472 **Figure 12.** Annual mean precipitation bias simulated over south-eastern Australia (WRF simulation
 473 inner domain) with respect to gridded observations for the period 1981-2010 for NARClIM2.0 RCMs
 474 (b-i) and NARClIM1.5 RCMs (j-m). Stippling and panel boundary colouring as per Fig. 3.

475

476 Switching driving reanalyses and simulating annual mean precipitation produces results that
 477 show consistent, large changes in RCM performances when using the newer ERA5 data, versus ERA-
 478 Interim. Forcing the NARClIM2.0 R1-R7 RCMs with ERA-Interim shows widespread, marked
 479 increases in bias for annual mean precipitation for 2016 (Fig 13b-i) relative to the preceding
 480 simulations using ERA5, such that the ensemble area-averaged mean absolute bias deteriorates to 8.02
 481 mm versus 3.97 mm, i.e. roughly doubling the bias magnitude. Conversely, forcing WRFJ-K-L with
 482 ERA5 improves the simulation of annual mean precipitation with all RCMs showing reductions in
 483 bias (Fig. 13j-m), such that the ensemble mean absolute bias decreases from 18.96 mm to 11.3 mm.
 484 These performance improvements are smaller in magnitude as compared to the degradation in
 performance when switching the driving data for the NARClIM2.0 R1-R7 RCMs.



485

486 **Figure 13.** Annual mean precipitation bias with respect to gridded observations for NARcliM2.0
 487 RCMs forced by ERA-Interim for 2016 plus two months spin-up starting in November 2015 (a-i), and
 488 corresponding NARcliM1.5 simulations for the same period forced by ERA5 (j-m).

489 **4. Discussion**

490 We have evaluated the capabilities of CORDEX-CMIP6 ERA5-driven RCMs in simulating the
 491 Australian climate and compared their performances to the previous generation of ERA-Interim
 492 forced RCMs produced for CORDEX-CMIP5. The newer generation of RCMs generally show
 493 improved simulations of maximum temperature and precipitation, but no improvements for minimum
 494 temperature. Several changes have been made to the design of the newer generation of RCMs,
 495 including different RCM physics parameterisations, model specifications, and the driving reanalysis is
 496 newer (ERA5). We found no evidence to suggest that the newer reanalysis contributes to the
 497 improvements in the simulation of maximum temperature by the ERA5 RCMs, whereas the opposite
 498 applies to the simulation of precipitation. This study focuses primarily on model evaluation with
 499 investigations of potential mechanisms underlying the varying performance profiles of the different
 500 RCM generations to be the subject of future research. This will be facilitated by the imminent
 501 publication of the NARcliM2.0 ERA5-RCM data.

502 **4.1 RCM performance evaluation**

503 As per the ERA-Interim driven RCMs, the NARcliM2.0 CORDEX-CMIP6 ERA5 RCMs are
 504 generally cold-biased for mean maximum temperature, however, their bias magnitudes are
 505 substantially lower relative to the CORDEX-CMIP5 ERA-Interim ensemble. The reductions in bias

506 magnitude for most CORDEX-CMIP6 ERA5-RCMs are especially marked for the convection-
507 permitting 4 km inner domain over south-eastern Australia. Similarly, these ERA5 RCMs show an
508 overall improved simulation of extreme maximum temperature over most of Australia relative to the
509 CORDEX-CMIP5 ERA-Interim forced RCMs. Improved simulation of mean and extreme maximum
510 temperature has important practical applications for climate impact assessment in Australia (e.g. Van
511 Oldenborgh et al., 2021; Di Virgilio et al., 2020a; Trancoso et al., 2020), as well as globally (e.g.
512 Vargas Zeppetello et al., 2022; Schleussner et al., 2016; Auffhammer et al., 2017).

513 Overall, CORDEX-CMIP6 ERA5-RCMs confer improvements in the simulation of mean
514 precipitation over south-eastern Australia relative to the CORDEX-CMIP5 ERA-Interim RCMs, with
515 two ERA5 RCMs in particular (R3, R4) showing considerable improvements over this region.
516 Improvements in the simulation of mean precipitation by CORDEX-CMIP6 ERA5 RCMs are even
517 more marked at convection-permitting scale over south-eastern Australia, i.e. the ERA5 ensemble
518 mean is 3.97 mm versus 18.96 mm for the ERA-Interim ensemble. Given the significant impacts of
519 drought and floods in Australia (González Tánago et al., 2016; Gu et al., 2020), this improvement in
520 mean precipitation simulation is an encouraging result. The performance in simulating extreme
521 precipitation over the Australian continent is comparable between the CORDEX-CMIP6 ERA5
522 RCMs and most CORDEX-CMIP5 ERA-Interim RCMs, except WRFSSWA, CCAM and CCLM
523 which show strong biases. However, at convection-permitting scale, some ERA5-RCMs show
524 improvements of around 10% in the simulation of extreme precipitation relative to the ERA-Interim
525 RCMs, except ERA5-R1 and R2 which are strongly wet-biased. For both mean and extreme
526 precipitation, ERA5 R1 and R2 are notable in that they are more wet-biased than the other ERA5
527 RCMs, especially over northern Australia where all other ERA5-RCMs contain a systematic dry-bias.
528 The only physics parameterisation common to both ERA5-R1 and R2 is their use of WSM6
529 microphysics, and no other RCMs assessed here use this physics scheme, with ERA5-R3-R7 using
530 Thompson microphysics. A previous assessment of the performance of different WRF
531 parameterisations for a one-way nested inner domain over central Europe observed that WSM6
532 increases annual wet bias relative to other microphysical schemes tested, including the Thomson
533 scheme (Varga and Breuer, 2020). Notably, marked dry-biases over the monsoonal north for several
534 ERA5-forced RCMs correspond with warm maximum temperature biases over this region shown by
535 several ERA5 RCMs.

536 Whilst the ERA5 RCMs confer improvements to the simulation of maximum temperature and
537 precipitation relative to ERA-Interim models, the simulation of minimum temperature for all
538 timescales and statistics shows no improvement over the Australian continent. Focusing specifically
539 on the WRF RCM configurations in the ERA-Interim ensemble, WRFJ and WRFK simulate both
540 mean and extreme minimum temperature more accurately than the ERA5-forced models, though in
541 some cases the differences are minimal. The exception to the above result is that some ERA5-RCMs

542 simulate mean minimum temperature more accurately along south-eastern coastlines at the 4 km
543 convection-permitting scale.

544 **4.2 ERA5 versus ERA-Interim evaluations: potential implications for** 545 **CMIP6-forced dynamical downscaling**

546 It could be expected that differences in the reanalysis data sets used to force the two generations of
547 WRF RCM ensemble contribute to the varying RCM performance profiles observed. ERA5 is a more
548 recent reanalysis which comprises a range of improvements over ERA-Interim, for instance, increased
549 resolutions spanning horizontal (~31 km versus ~79 km), vertical (137 levels to 0.01 hPa versus 60 to
550 0.1 hPa), and temporal dimensions (hourly versus 6-hourly), among other features such as improved
551 parameterisations (Hersbach et al., 2020). ERA5 has been shown to confer improvements over ERA-
552 Interim in the simulation of processes such as convective updrafts, tropical cyclones, and other meso-
553 to synoptic-scale atmospheric features (Hoffmann et al., 2019) and in some cases the simulation of
554 rainfall (e.g. Nogueira, 2020). Our investigation into whether differences in the driving reanalyses
555 contribute to the varying RCM performances observed between the two WRF RCM ensembles
556 involved two assessments: i) comparisons of the ERA5 and ERA-Interim reanalyses against AGCD
557 observations to assess their degree of bias; ii) fourteen-month simulations where otherwise identically
558 parameterised NARClIM2.0 R1-R7 RCMs were forced by ERA-Interim as opposed to ERA5, and
559 similarly the WRFJ-K-L RCMs were forced with ERA5 instead of ERA-Interim.

560 Comparison of ERA5 and ERA-Interim reanalysis data versus observations for mean
561 maximum and minimum temperature and precipitation shows the expected results, i.e. that ERA5 data
562 are closer to observations relative to ERA-Interim for all variables, especially for mean precipitation.
563 Percentage differences in area-averaged mean absolute bias for annual means range from 25% for
564 minimum temperature to 65% for precipitation, also noting that performances during summer were
565 more divergent than at annual timescales. Therefore, in terms of the underlying reanalysis data used to
566 force the different WRF RCMs evaluated, ERA5 shows improvements relative to ERA-Interim.
567 Additionally, these improvements are of larger magnitude for mean precipitation than they are for
568 mean maximum and minimum temperature.

569 For the 1-year simulations where the driving reanalyses are switched, using ERA5 over ERA-
570 Interim gives a large performance improvement in the simulation of annual mean precipitation for the
571 CORDEX-CMIP5 WRFJ-K-L RCMs. In contrast, using ERA5 over ERA-Interim as the driving data
572 generally produces RCM performance degradations for both annual mean maximum and minimum
573 temperature. That is, a superior simulation of mean maximum and minimum temperature is generally
574 obtained for both generations of WRF RCM by using ERA-Interim instead of ERA5. These results
575 suggest that, at least for the different generations of WRF RCM assessed here in these 1-year
576 experiments, using a more accurate driving reanalysis for dynamical downscaling over this region

577 does not guarantee an enhanced simulation for all climatic variables. This result is surprising and
578 warrants further investigation. However, this finding suggests that the parameterisations and design
579 features of the WRF RCMs assessed play important roles in determining how well these RCMs
580 simulate mean maximum and minimum temperature. Consequently, the improved simulations of
581 maximum temperature by CORDEX-CMIP6 ERA5-RCMs relative to CORDEX-CMIP5 ERA-
582 Interim-RCMs are more attributable to model design choices, such as physics parameterisations
583 and/or improved resolution, rather than to the driving reanalyses per se. Additionally, that the
584 CORDEX-CMIP6 ERA5-forced R1-R7 RCMs do not improve the simulation of minimum
585 temperature relative to CORDEX-CMIP5 ERA-Interim-forced RCMs is not attributable to the change
586 from ERA-Interim to ERA5 as the driving reanalysis, rather, to aspect(s) of model
587 parameterisation/design. Conversely, substantial improvements in simulating mean precipitation by
588 CORDEX-CMIP6 ERA5-RCMs relative to CORDEX-CMIP5 ERA-Interim-forced RCMs appear (at
589 least in part) due to the improvements to the ERA5 driving reanalysis. There are limitations to these
590 comparative analyses switching the driving data, such as simulating for fourteen months and not a
591 climatological period. Nevertheless, the present evaluations suggest that whether CORDEX-CMIP6
592 dynamical downscaling of CMIP6 GCMs produces improved regional climate simulations relative to
593 CORDEX-CMIP5 downscaling may depend in large part, at least for some variables/statistics, on
594 RCM parameterisations and other design choices. However, the generality of these findings to other
595 RCM types, configurations, study domains, and downscaling experiments warrants further research as
596 these results may be specific to the WRF RCMs and domains assessed here.

597 **4.3 ERA5-R1-R7 and CMIP6-forced dynamical downscaling**

598 Although a single 'all-round' best-performing ERA5-RCM configuration cannot be selected, the RCM
599 performances for the climate variables and statistics assessed here yield some insights if selecting a
600 subset of ERA5-RCM configurations for subsequent CMIP6-forced downscaling. Overall, ERA5-R1
601 provides a good simulation of both mean and extreme maximum temperature and is broadly
602 comparable to the other ERA5-RCMs with respect to minimum temperature. However, its simulation
603 of mean and extreme precipitation is relatively poor as compared to most ERA5-RCMs. ERA5-R2 has
604 an unusual performance profile relative to the other ERA5-RCMs. Although ERA5-R2 shows
605 generally good performance for minimum temperature, extreme maximum temperature and
606 precipitation, it shows poor performance for mean maximum temperature in that is considerably more
607 cold-biased than the other ERA5-RCMs. ERA5-R2 is the only ERA5-forced RCM configuration in
608 this ensemble to use Kain-Fritsch cumulus physics, and it shows mean maximum temperature biases
609 of roughly similar magnitude and spatial pattern as the ERA-Interim WRFJ and WRFK RCMs which
610 also use the same scheme. However, ERA5-R2 also generates a strong mean maximum temperature
611 cold bias over south-eastern Australia at the 4 km convection-permitting scale which does not use

612 cumulus parameterisation. ERA5-R3 shows good performance for mean minimum temperature and
613 mean precipitation and reasonable performance for mean maximum temperature. The performance of
614 ERA5-R4 is broadly similar to ERA5-R3, but it has substantially inferior performance versus ERA5-
615 R3 for maximum and minimum temperature extremes. ERA5-R5 shows consistently good
616 performance for maximum temperature. The performance of ERA5-R5 in simulating precipitation
617 over Australia at 20 km resolution is not impressive versus the other ERA5-RCMs and it shows strong
618 dry biases over northern Australia. However, ERA5-R5 is the best-performing model in this ensemble
619 for mean precipitation at the 4 km convection permitting scale over south-eastern Australia. Both
620 ERA5-R6 and ERA5-R7 frequently show the strongest biases, typically over large regions such as
621 eastern Australia for both temperature variables, and over northern Australia for precipitation. As
622 such, they are the poorest performers overall in this ERA5 ensemble, with performance for extreme
623 minimum temperature often being particularly poor.

624 From the specific perspective of the ERA5-RCM performances, and based on the present
625 evaluations, overall ERA5-R3 and ERA5-R5 may be considered favourable RCM configurations for
626 CMIP6-forced dynamical downscaling. However, as noted, some other ERA5 RCM configurations
627 show good performance for specific variables and statistics, and thus could warrant inclusion in a
628 larger ensemble and/or one adopting a sparse matrix approach (Christensen and Kjellström, 2020).

629 **5. Conclusions**

630 This study forms the first part of a series of simulations for the CORDEX Australasia domain,
631 wherein we document model performances of ERA5 reanalysis-forced RCMs, and this is the first set
632 of simulations as required by the CORDEX-CMIP6 framework. We compared our results against
633 ERA-Interim driven simulations which was part of the CORDEX-CMIP5 framework. While model
634 versions and physics options were different between these two generations of reanalysis-forced RCM
635 simulations, overall, our results show the NARClIM2.0 ERA5-forced RCMs confer improved
636 simulations for maximum temperature and precipitation, but not for minimum temperature.

637 The simulation of precipitation by the NARClIM2.0 RCMs show several improvements at the
638 4 km convection permitting scale relative to the 20 km outer domain. For example, dry biases are
639 reduced for the convection-permitting domain where convection is represented explicitly, relative to
640 the 20 km outer domain which uses a convective parametrisation. Convection schemes can be a
641 source of deficiencies in RCM simulations of precipitation (e.g. Jones and Randall, 2011). It may be
642 expected that the improved representation of convection for the 4 km domain may positively
643 influence the simulation of high-impact phenomena such as short-duration precipitation extremes.
644 Nevertheless, our results for the CORDEX-Australasia domain suggest that the choice of
645 microphysics scheme is important, especially for precipitation extremes.

646 Whilst ERA5 reanalysis data show better representations of the observed Australian climate
647 than ERA-Interim, only improvements in the simulation of mean precipitation by the CORDEX-
648 CMIP6 ERA5-RCMs appear at least partly attributable to the increased accuracy of ERA5 driving
649 reanalyses. Conversely, the change in driving reanalysis from ERA-Interim to ERA5 is not a major
650 factor underlying improvements in the simulation of maximum temperature by the CORDEX-CMIP6
651 RCMs assessed, suggesting that their performance improvements are more attributable to changes in
652 RCM parameterisation and design. The different land surface schemes (e.g. Noah-Unified versus
653 Noah-MP) likely play a role in RCM skill in simulating maximum temperature, as well as changing
654 the land surface feedback (via soil moisture) to the simulation of precipitation – these possibilities
655 require more extensive analysis to investigate. Equally, differences in the underlying driving reanalyses
656 do not explain the absence of overall improvements in the simulation of minimum temperature by the
657 newer CORDEX-CMIP6 RCMs. It is important to be cautious of generalising the present results to
658 other regions globally, as region-specific RCM optimisation is necessary.

659 Our present focus was to evaluate the performances of the different RCM generations
660 assessed here. Future work will explore other topics, such as the potential influences of the different
661 RCM physics configurations and their associated biases on the nature of the future change signals in
662 subsequent CMIP6 GCM-forced simulations, e.g. when holding the driving GCM data constant.
663 Additionally, future model-intercomparison studies that compare biases between the different RCMs
664 contributing to CORDEX-Australasia will be valuable.

665 Results presented here are relevant for other CORDEX-CMIP6/CORDEX2 modelling
666 projects. Maximum temperature and precipitation are important inputs to climate impact assessments
667 in Australia, and globally. The improvements in simulating maximum temperature and precipitation
668 conferred by CORDEX-CMIP6 ERA5-forced RCMs evaluated here indicate that using a subset of the
669 RCMs in this ensemble for future CMIP6-forced downscaling over CORDEX Australasia could yield
670 benefits in simulating regional climate.

671 **6. Code Availability**

672 The Weather Research and Forecasting (WRF) version 4.1.2 and all model configuration files used
673 in this study are available on Zenodo at: <https://doi.org/10.5281/zenodo.11189898>

674 **7. Data Availability**

675 Data for the seven CORDEX-CMIP6 ERA5-forced R1-R7 RCMs are being made available via
676 [National Computing Infrastructure](#) (NCI). WRF namelist settings for the CORDEX-CMIP6 ERA5-
677 forced RCMs R1-R7 are shown in Supplementary Material Fig. S32. Data for the three ERA-Interim
678 forced WRFJ-K-L RCMs are available via the [New South Wales Climate Data Portal](#) and [CORDEX-](#)

679 [DKRZ](#), and data for ERA-Interim forced CCAM, CCLM and WRFSSWA are available via
680 [CORDEX-DKRZ](#).

681 **8. Author Contribution**

682 GDV and JPE designed the models and the simulations. FJ, ET, JA and CT setup the models and
683 conducted the model simulations with contributions from JPE, JK, GDV and YL. GDV prepared the
684 manuscript with contributions from all co-authors.

685 **9. Competing Interests**

686 The authors declare that they have no conflict of interest, noting that JK has been a Topic Editor of
687 Geoscientific Model Development from 2015 to 2024.

688 **10. Funding**

689 This research was supported by the New South Wales Department of Climate Change, Energy, the
690 Environment and Water as part of the NARClM2.0 dynamical downscaling project contributing to
691 CORDEX Australasia. Funding was provided by the NSW Climate Change Fund, the NSW Climate
692 Change Adaptation Strategy Program, and the ACT, SA, WA and VIC Governments for the NSW and
693 Australia Regional Climate Modelling (NARClM) Project. This research was undertaken with the
694 assistance of resources and services from the National Computational Infrastructure (NCI), which is
695 supported by the Australian Government.

696 Jason P. Evans acknowledges the support of the Australian Research Council Centre of Excellence for
697 Climate Extremes (CE170100023) and the Climate Systems Hub of the Australian Governments
698 National Environmental Science Program.

699 **11. Acknowledgements**

700 All authors thank the reviewers for their thoughtful and insightful feedback on this manuscript, and
701 the Editor at Geoscientific Model Development for handling the peer review process of this
702 manuscript.

703 **12. References**

704 Auffhammer, M., Baylis, P., and Hausman, C. H.: Climate change is projected to have severe impacts
705 on the frequency and intensity of peak electricity demand across the United States,

706 Proceedings of the National Academy of Sciences, 114, 1886-1891,
707 doi:10.1073/pnas.1613193114, 2017.

708 Bucchignani, E., Mercogliano, P., Rianna, G., and Panitz, H. J.: Analysis of ERA-Interim-driven
709 COSMO-CLM simulations over Middle East - North Africa domain at different spatial
710 resolutions, *International Journal of Climatology*, 36, 3346-3369, 10.1002/joc.4559, 2016.

711 Bureau of Meteorology: Australian Gridded Climate Data (AGCD) ; v2.0.0 Snapshot (1900-01-01 to
712 2020-05-31), 2020.

713 Bureau of Meteorology, Annual climate statement 2016, last access: February 15 2024.

714 Chou, M. D., Suarez, M. J., Liang, X. Z., and Yan, M. M. H.: A thermal infrared radiation
715 parameterization for atmospheric studies, NASA Tech. Memo. NASA/TM-2001-104606, 19,
716 68 pp. <https://ntrs.nasa.gov/citations/20010072848>, 2001.

717 Christensen, O. B. and Kjellström, E.: Partitioning uncertainty components of mean climate and
718 climate change in a large ensemble of European regional climate model projections, *Climate
719 Dynamics*, 54, 4293-4308, 10.1007/s00382-020-05229-y, 2020.

720 Dee, D. P., Uppala, S. M., Simmons, A. J., Berrisford, P., Poli, P., Kobayashi, S., Andrae, U.,
721 Balmaseda, M. A., Balsamo, G., Bauer, P., Bechtold, P., Beljaars, A. C. M., van de Berg, L.,
722 Bidlot, J., Bormann, N., Delsol, C., Dragani, R., Fuentes, M., Geer, A. J., Haimberger, L.,
723 Healy, S. B., Hersbach, H., Hólm, E. V., Isaksen, L., Kållberg, P., Köhler, M., Matricardi, M.,
724 McNally, A. P., Monge-Sanz, B. M., Morcrette, J. J., Park, B. K., Peubey, C., de Rosnay, P.,
725 Tavolato, C., Thépaut, J. N., and Vitart, F.: The ERA-Interim reanalysis: configuration and
726 performance of the data assimilation system, *Quarterly Journal of the Royal Meteorological
727 Society*, 137, 553-597, 10.1002/qj.828, 2011.

728 Di Luca, A., de Elia, R., and Laprise, R.: Potential for added value in precipitation simulated by high-
729 resolution nested Regional Climate Models and observations, *Clim. Dyn.*, 38, 1229-1247,
730 10.1007/s00382-011-1068-3, 2012.

731 Di Virgilio, G., Evans, J. P., Clarke, H., Sharples, J., Hirsch, A. L., and Hart, M. A.: Climate Change
732 Significantly Alters Future Wildfire Mitigation Opportunities in Southeastern Australia,
733 *Geophys. Res. Lett.*, 47, e2020GL088893, <https://doi.org/10.1029/2020GL088893>, 2020a.

734 Di Virgilio, G., Evans, J. P., Di Luca, A., Grose, M. R., Round, V., and Thatcher, M.: Realised added
735 value in dynamical downscaling of Australian climate change, *Clim. Dyn.*, 54, 4675-4692,
736 10.1007/s00382-020-05250-1, 2020b.

737 Di Virgilio, G., Evans, J. P., Di Luca, A., Olson, R., Argüeso, D., Kala, J., Andrys, J., Hoffmann, P.,
738 Katzfey, J. J., and Rockel, B.: Evaluating reanalysis-driven CORDEX regional climate
739 models over Australia: model performance and errors, *Clim. Dyn.*, 53, 2985-3005,
740 10.1007/s00382-019-04672-w, 2019.

741 Di Virgilio, G., Evans, J., Ji, F., Tam, E., Kala, J., Andrys, J., Thomas, C., Choudhury, D., Rocha, C.,
742 White, S., Li, Y., El Rafei, M., Goyal, R., Riley, M., and Lingala, J.: Design, evaluation and

743 future projections of the NARClIM2.0 CORDEX-CMIP6 Australasia regional climate
744 ensemble, *Geosci. Model Dev. Discuss.*, 2024, 1-48, <https://doi.org/10.5194/gmd-2024-87>,
745 2024.

746 Ekström, M., Grose, M. R., and Whetton, P. H.: An appraisal of downscaling methods used in climate
747 change research, *Wiley Interdisciplinary Reviews: Climate Change*, 6, 301-319,
748 10.1002/wcc.339, 2015.

749 Evans, A., Jones, D., Lellyett, S., and Smalley, R.: An Enhanced Gridded Rainfall Analysis Scheme
750 for Australia, Australian Bureau of Meteorology, 2020.

751 Evans, J. P., Ji, F., Lee, C., Smith, P., Argüeso, D., and Fita, L.: Design of a regional climate
752 modelling projection ensemble experiment - NARClIM, *Geosci. Model Dev.*, 7, 621-629,
753 10.5194/gmd-7-621-2014, 2014.

754 Eyring, V., Bony, S., Meehl, G. A., Senior, C. A., Stevens, B., Stouffer, R. J., and Taylor, K. E.:
755 Overview of the Coupled Model Intercomparison Project Phase 6 (CMIP6) experimental
756 design and organization, *Geosci. Model Dev.*, 9, 1937-1958, 10.5194/gmd-9-1937-2016,
757 2016.

758 Giorgi, F.: Regional climate modeling: Status and perspectives, *J. Phys. IV*, 139, 101-118,
759 10.1051/jp4:2006139008, 2006.

760 Giorgi, F.: Thirty Years of Regional Climate Modeling: Where Are We and Where Are We Going
761 next?, *Journal of Geophysical Research: Atmospheres*, 124, 5696-5723,
762 10.1029/2018jd030094, 2019.

763 Giorgi, F. and Bates, G. T.: The Climatological Skill of a Regional Model over Complex Terrain,
764 *Monthly Weather Review*, 117, 2325-2347, 10.1175/1520-0493(1989)117, 1989.

765 Giorgi, F., Jones, C., and Asrar, G.: Addressing climate information needs at the regional level: The
766 CORDEX framework, *WMO Bulletin*, 53, 175–183, 2009.

767 González Tánago, I., Urquijo, J., Blauhut, V., Villarroya, F., and De Stefano, L.: Learning from
768 experience: a systematic review of assessments of vulnerability to drought, *Nat. Hazards*, 80,
769 951-973, 10.1007/s11069-015-2006-1, 2016.

770 Grose, M. R., Narsey, S., Delage, F. P., Dowdy, A. J., Bador, M., Boschhat, G., Chung, C., Kajtar, J.
771 B., Rauniyar, S., Freund, M. B., Lyu, K., Rashid, H., Zhang, X., Wales, S., Trenham, C.,
772 Holbrook, N. J., Cowan, T., Alexander, L., Arblaster, J. M., and Power, S.: Insights From
773 CMIP6 for Australia's Future Climate, *Earth's Future*, 8, e2019EF001469,
774 <https://doi.org/10.1029/2019EF001469>, 2020.

775 Grose, M., Narsey, S., Trancoso, R., Mackallah, C., Delage, F., Dowdy, A., Di Virgilio, G.,
776 Watterson, I., Dobrohotoff, P., Rashid, H. A., Rauniyar, S., Henley, B., Thatcher, M., Syktus,
777 J., Abramowitz, G., Evans, J. P., Su, C.-H., and Takbash, A.: A CMIP6-based multi-model
778 downscaling ensemble to underpin climate change services in Australia, *Climate Services*, 30,
779 100368, <https://doi.org/10.1016/j.cliser.2023.100368>, 2023.

780 Gu, X. H., Zhang, Q., Li, J. F., Liu, J. Y., Xu, C. Y., and Sun, P.: The changing nature and projection
781 of floods across Australia, *J. Hydrol.*, 584, 10.1016/j.jhydrol.2020.124703, 2020.

782 Gutowski, W. J., Giorgi, F., Timbal, B., Frigon, A., Jacob, D., Kang, H. S., Raghavan, K., Lee, B.,
783 Lennard, C., Nikulin, G., O'Rourke, E., Rixen, M., Solman, S., Stephenson, T., and Tangang,
784 F.: WCRP COordinated Regional Downscaling EXperiment (CORDEX): a diagnostic MIP
785 for CMIP6, *Geoscientific Model Development*, 9, 4087-4095, 10.5194/gmd-9-4087-2016,
786 2016.

787 Hersbach, H., Bell, B., Berrisford, P., Hirahara, S., Horányi, A., Muñoz-Sabater, J., Nicolas, J.,
788 Peubey, C., Radu, R., Schepers, D., Simmons, A., Soci, C., Abdalla, S., Abellan, X.,
789 Balsamo, G., Bechtold, P., Biavati, G., Bidlot, J., Bonavita, M., De Chiara, G., Dahlgren, P.,
790 Dee, D., Diamantakis, M., Dragani, R., Flemming, J., Forbes, R., Fuentes, M., Geer, A.,
791 Haimberger, L., Healy, S., Hogan, R. J., Hólm, E., Janisková, M., Keeley, S., Laloyaux, P.,
792 Lopez, P., Lupu, C., Radnoti, G., de Rosnay, P., Rozum, I., Vamborg, F., Villaume, S., and
793 Thépaut, J.-N.: The ERA5 global reanalysis, *Quarterly Journal of the Royal Meteorological
794 Society*, 146, 1999-2049, <https://doi.org/10.1002/qj.3803>, 2020.

795 Hoffmann, L., Gunther, G., Li, D., Stein, O., Wu, X., Griessbach, S., Heng, Y., Konopka, P., Muller,
796 R., Vogel, B., and Wright, J. S.: From ERA-Interim to ERA5: the considerable impact of
797 ECMWF's next-generation reanalysis on Lagrangian transport simulations, *Atmos. Chem.
798 Phys.*, 19, 3097-3124, 10.5194/acp-19-3097-2019, 2019.

799 Hong, S.-Y., Noh, Y., and Dudhia, J.: A New Vertical Diffusion Package with an Explicit Treatment
800 of Entrainment Processes, *Monthly Weather Review*, 134, 2318-2341,
801 <https://doi.org/10.1175/MWR3199.1>, 2006.

802 Hong, S. Y. and Lim, J.-O. J.: The WRF Single-Moment 6-Class Microphysics Scheme (WSM6),
803 *Asia-Pac. J. Atmos. Sci.*, 42, 129-151, 2006.

804 Howard, E., Su, C. H., Stassen, C., Naha, R., Ye, H., Pepler, A., Bell, S. S., Dowdy, A. J., Tucker, S.
805 O., and Franklin, C.: Performance and process-based evaluation of the BARPA-R
806 Australasian regional climate model version 1, *Geosci. Model Dev.*, 17, 731-757,
807 10.5194/gmd-17-731-2024, 2024.

808 Hsiang, S., Kopp, R., Jina, A., Rising, J., Delgado, M., Mohan, S., Rasmussen, D. J., Muir-Wood, R.,
809 Wilson, P., Oppenheimer, M., Larsen, K., and Houser, T.: Estimating economic damage from
810 climate change in the United States, *Science*, 356, 1362-1368, 10.1126/science.aal4369, 2017.

811 Iacono, M. J., Delamere, J. S., Mlawer, E. J., Shephard, M. W., Clough, S. A., and Collins, W. D.:
812 Radiative forcing by long-lived greenhouse gases: Calculations with the AER radiative
813 transfer models, *Journal of Geophysical Research: Atmospheres*, 113,
814 <https://doi.org/10.1029/2008JD009944>, 2008.

815 IPCC: Climate Change 2021: The Physical Science Basis. Contribution of Working Group I to the
816 Sixth Assessment Report of the Intergovernmental Panel on Climate Change, Cambridge
817 University Press, 2021.

818 Janjić, Z. I.: Comments on “Development and Evaluation of a Convection Scheme for Use in Climate
819 Models”, *Journal of the Atmospheric Sciences*, 57, 3686-3686, [https://doi.org/10.1175/1520-
820 0469\(2000\)057<3686:CODAEO>2.0.CO;2](https://doi.org/10.1175/1520-0469(2000)057<3686:CODAEO>2.0.CO;2), 2000.

821 Jones, T. R. and Randall, D. A.: Quantifying the limits of convective parameterizations, *Journal of
822 Geophysical Research: Atmospheres*, 116, <https://doi.org/10.1029/2010JD014913>, 2011.

823 Kain, J. S.: The Kain-Fritsch convective parameterization: An update, *Journal of Applied
824 Meteorology*, 43, 170-181, 10.1175/1520-0450, 2004.

825 Laprise, R.: Regional climate modelling, *J. Comput. Phys.*, 227, 3641-3666,
826 10.1016/j.jcp.2006.10.024, 2008.

827 Ma, M. N., Ou, T. H., Liu, D. Q., Wang, S. Y., Fang, J., and Tang, J. P.: Summer regional climate
828 simulations over Tibetan Plateau: from gray zone to convection permitting scale, *Clim. Dyn.*,
829 10.1007/s00382-022-06314-0, 2022.

830 McGregor, J. L. and Dix, M. R.: An updated description of the Conformal-Cubic atmospheric model,
831 *High Resolution Numerical Modelling of the Atmosphere and Ocean*, Springer, New York,
832 51-75 pp., 10.1007/978-0-387-49791-4_4, 2008.

833 Nakanishi, M. and Niino, H.: Development of an Improved Turbulence Closure Model for the
834 Atmospheric Boundary Layer, *Journal of the Meteorological Society of Japan. Ser. II*, 87,
835 895-912, 10.2151/jmsj.87.895, 2009.

836 Nishant, N., Evans, J. P., Di Virgilio, G., Downes, S. M., Ji, F., Cheung, K. K. W., Tam, E., Miller, J.,
837 Beyer, K., and Riley, M. L.: Introducing NARCLIM1.5: Evaluating the Performance of
838 Regional Climate Projections for Southeast Australia for 1950–2100, *Earth's Future*, 9,
839 e2020EF001833, <https://doi.org/10.1029/2020EF001833>, 2021.

840 Niu, G.-Y., Yang, Z.-L., Mitchell, K. E., Chen, F., Ek, M. B., Barlage, M., Kumar, A., Manning, K.,
841 Niyogi, D., Rosero, E., Tewari, M., and Xia, Y.: The community Noah land surface model
842 with multiparameterization options (Noah-MP): 1. Model description and evaluation with
843 local-scale measurements, *Journal of Geophysical Research: Atmospheres*, 116,
844 10.1029/2010jd015139, 2011.

845 Nogueira, M.: Inter-comparison of ERA-5, ERA-interim and GPCP rainfall over the last 40 years:
846 Process-based analysis of systematic and random differences, *J. Hydrol.*, 583,
847 10.1016/j.jhydrol.2020.124632, 2020.

848 Panitz, H.-J., Dosio, A., Büchner, M., Lüthi, D., and Keuler, K.: COSMO-CLM (CCLM) climate
849 simulations over CORDEX-Africa domain: analysis of the ERA-Interim driven simulations at
850 0.44° and 0.22° resolution, *Clim. Dyn.*, 42, 3015-3038, 10.1007/s00382-013-1834-5, 2014.

851 Perkins, S. E., Pitman, A. J., Holbrook, N. J., and McAneney, J.: Evaluation of the AR4 climate
852 models' simulated daily maximum temperature, minimum temperature, and precipitation over
853 Australia using probability density functions, *J. Clim.*, 20, 4356-4376, 10.1175/jcli4253.1,
854 2007.

855 Pleim, J. E.: A Combined Local and Nonlocal Closure Model for the Atmospheric Boundary Layer.
856 Part I: Model Description and Testing, *J. Appl. Meteorol. Climatol.*, 46, 1383-1395,
857 <https://doi.org/10.1175/JAM2539.1>, 2007.

858 Reder, A., Raffa, M., Padulano, R., Rianna, G., and Mercogliano, P.: Characterizing extreme values
859 of precipitation at very high resolution: An experiment over twenty European cities, *Weather
860 and Climate Extremes*, 35, 10.1016/j.wace.2022.100407, 2022.

861 Rockel, B., Will, A., and Hense, A.: The Regional Climate Model COSMO-CLM(CCLM), *Meteorol.
862 Z.*, 17, 347-348, 10.1127/0941-2948/2008/0309, 2008.

863 Schleussner, C. F., Lissner, T. K., Fischer, E. M., Wohland, J., Perrette, M., Golly, A., Rogelj, J.,
864 Childers, K., Schewe, J., Frieler, K., Mengel, M., Hare, W., and Schaeffer, M.: Differential
865 climate impacts for policy-relevant limits to global warming: the case of 1.5 °C and 2 °C,
866 *Earth Syst. Dynam.*, 7, 327-351, 10.5194/esd-7-327-2016, 2016.

867 Skamarock, W. C., Klemp, J. B., Dudhia, J., Gill, D. O., Barker, D. M., Wang, W., and Powers, J. G.:
868 A description of the Advanced Research WRF Version 3. NCAR Tech Note NCAR/TN-
869 475+STR. NCAR, Boulder, CO, 2008.

870 Stouffer, R. J., Eyring, V., Meehl, G. A., Bony, S., Senior, C., Stevens, B., and Taylor, K. E.: CMIP5
871 Scientific Gaps and Recommendations for CMIP6, *Bulletin of the American Meteorological
872 Society*, 98, 95-105, 10.1175/bams-d-15-00013.1, 2017.

873 Tebaldi, C., Arblaster, J. M., and Knutti, R.: Mapping model agreement on future climate projections,
874 *Geophys. Res. Lett.*, 38, doi:10.1029/2011GL049863, 2011.

875 Tewari, M., Wang, W., Dudhia, J., LeMone, M. A., Mitchell, K., Ek, M., Gayno, G., Wegiel, J., and
876 Cuenca, R.: Implementation and verification of the united NOAH land surface model in the
877 WRF model, 11-15 pp.2016.

878 Thompson, G., Field, P. R., Rasmussen, R. M., and Hall, W. D.: Explicit Forecasts of Winter
879 Precipitation Using an Improved Bulk Microphysics Scheme. Part II: Implementation of a
880 New Snow Parameterization, *Monthly Weather Review*, 136, 5095-5115,
881 <https://doi.org/10.1175/2008MWR2387.1>, 2008.

882 Tiedtke, M.: A Comprehensive Mass Flux Scheme for Cumulus Parameterization in Large-Scale
883 Models, *Monthly Weather Review*, 117, 1779-1800, 10.1175/1520-
884 0493(1989)117<1779:acmfsf>2.0.co;2, 1989.

885 Torma, C., Giorgi, F., and Coppola, E.: Added value of regional climate modeling over areas
886 characterized by complex terrain—Precipitation over the Alps, *Journal of Geophysical
887 Research: Atmospheres*, 120, 3957-3972, 10.1002/2014JD022781, 2015.

888 Trancoso, R., Syktus, J., Toombs, N., Ahrens, D., Wong, K. K.-H., and Pozza, R. D.: Heatwaves
889 intensification in Australia: A consistent trajectory across past, present and future, *Sci. Total*
890 *Environ.*, 742, 140521, <https://doi.org/10.1016/j.scitotenv.2020.140521>, 2020.

891 Van de Walle, J., Thiery, W., Brousse, O., Souverijns, N., Demuzere, M., and van Lipzig, N. P. M.: A
892 convection-permitting model for the Lake Victoria Basin: evaluation and insight into the
893 mesoscale versus synoptic atmospheric dynamics, *Clim. Dyn.*, 54, 1779-1799,
894 10.1007/s00382-019-05088-2, 2020.

895 van Oldenborgh, G. J., Krikken, F., Lewis, S., Leach, N. J., Lehner, F., Saunders, K. R., van Weele,
896 M., Haustein, K., Li, S., Wallom, D., Sparrow, S., Arrighi, J., Singh, R. K., van Aalst, M. K.,
897 Philip, S. Y., Vautard, R., and Otto, F. E. L.: Attribution of the Australian bushfire risk to
898 anthropogenic climate change, *Nat. Hazards Earth Syst. Sci.*, 21, 941-960, 10.5194/nhess-21-
899 941-2021, 2021.

900 Varga, A. J. and Breuer, H.: Sensitivity of simulated temperature, precipitation, and global radiation
901 to different WRF configurations over the Carpathian Basin for regional climate applications,
902 *Clim. Dyn.*, 55, 2849-2866, 10.1007/s00382-020-05416-x, 2020.

903 Vargas Zeppetello, L. R., Raftery, A. E., and Battisti, D. S.: Probabilistic projections of increased heat
904 stress driven by climate change, *Communications Earth & Environment*, 3, 183,
905 10.1038/s43247-022-00524-4, 2022.

906 Zhou, X., Yang, K., Ouyang, L., Wang, Y., Jiang, Y. Z., Li, X., Chen, D. L., and Prein, A.: Added
907 value of kilometer-scale modeling over the third pole region: a CORDEX-CPTP pilot study,
908 *Clim. Dyn.*, 57, 1673-1687, 10.1007/s00382-021-05653-8, 2021.